

Banner appropriate to article type will appear here in typeset article

# Internally heated convection with rotation: bounds and scaling laws for heat transport

Ali Arslan<sup>†</sup>

Institute of Geophysics, ETH Zürich, Zürich, CH-8092, Switzerland

(Received xx; revised xx; accepted xx)

This work investigates heat transport in rotating internally heated convection, for a horizontally periodic fluid between parallel plates under no-slip and isothermal boundary conditions. The main results are the proof of bounds on the mean temperature,  $\overline{\langle T \rangle}$ , and the heat flux out of the bottom boundary,  $\mathcal{F}_B$  at infinite Prandtl numbers where the Prandtl number is the nondimensional ratio of viscous to thermal diffusion. The lower bounds are functions of a Rayleigh number quantifying the ratio of internal heating to diffusion and the Ekman number,  $E$ , which quantifies the ratio of viscous diffusion to rotation. We utilise two different estimates on the vertical velocity,  $w$ , one pointwise in the domain (Yan 2004, *J. Math. Phys.*, vol.45(7), pp.2718-2743) and the other an integral estimate over the domain (Constantin *et al.* 1999, *Phys. D: Non. Phen.*, vol. 125, pp. 275-284), resulting in bounds valid for different regions of buoyancy-to-rotation dominated convection. Furthermore, we demonstrate that similar to rotating Rayleigh-Bénard convection, for small  $E$ , the critical Rayleigh number for the onset of convection asymptotically scales as  $E^{-4/3}$ . This result is combined with heuristic arguments for internally heated and rotating convection to arrive at scaling laws for  $\overline{\langle T \rangle}$  and  $\mathcal{F}_B$  valid for arbitrary Prandtl numbers.

**Key words:** turbulent convection, variational methods

## 1. Introduction

Heat transport by turbulent convection remains a pertinent area of research in both astrophysical and geophysical fluid dynamics. While boundary-forced thermal convection has been extensively studied, convection driven by internal heating has been relatively overlooked (Doering 2020). Nevertheless, internally heated convection (IHC) plays a significant role within planetary bodies, such as in the Earth's mantle and core, where the radioactive decay of isotopes and secular cooling drive fluid motion (Schubert *et al.* 2001; Schubert 2015). Similarly, for stars, convective zones are driven by radiation from nuclear fusion (Schumacher & Sreenivasan 2020) and supernovae are modelled as fluids heated internally by neutrinos (Herant *et al.* 1994; Radice *et al.* 2016). Moreover, stars and planets are rotating bodies and the Coriolis force significantly affects the flow dynamics (Greenspan 1968).

Studying rotating turbulent convection is challenging because experiments and numerical

<sup>†</sup> Email address for correspondence: ali.arslan@erdw.ethz.ch

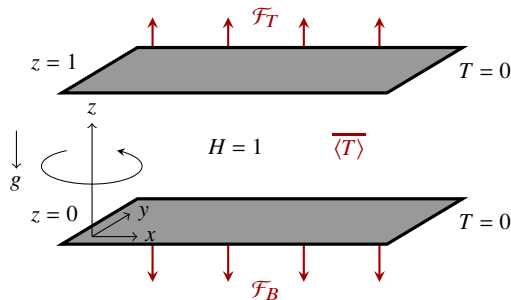


Figure 1: A non-dimensional schematic diagram for rotating uniform internally heated convection. The upper and lower plates are at the same temperature, and the domain is periodic in the  $x$  and  $y$  directions and rotates about the  $z$  axis.  $\mathcal{F}_B$  and  $\mathcal{F}_T$  are the mean heat fluxes out the bottom and top plates,  $\overline{\langle T \rangle}$  the mean temperature, and  $g$  is the acceleration due to gravity.

simulations cannot reach parameter values of interest (Glatzmaier 2013). For example, in planetary mantles, the Prandtl number,  $Pr$ , the non-dimensional number quantifying the ratio of the viscous and thermal diffusivity, reaches values of  $10^{23}$ , while the Rayleigh number,  $R$ , quantifying the ratio of thermal forcing to diffusion is at least  $10^6$  (Mulyukova & Bercovici 2020). In planetary cores, the Rayleigh number could be as high as  $10^{26}$  (Schubert 2015). Furthermore, the Ekman number,  $E$ , representing the viscous to rotational forces, is estimated to be  $10^{-15}$  in the Earth's core (Jones & Schubert 2015).

An alternative route for inquiry is a mathematically rigorous study of the equations describing rotating convection. Of interest is the regime where the solutions of the governing equations are turbulent, and a key question is on the long-time behaviour of the mean quantities of the flow as a function of the control parameters ( $Pr$ ,  $R$ ,  $E$ ). In this study, we employ the *background field method* (Doering & Constantin 1992, 1994; Constantin & Doering 1995; Doering & Constantin 1996) to study the mean heat transport in IHC subject to rotation between parallel plates with isothermal and no-slip boundary conditions (fig. 1). Unlike turbulent convection driven by boundary heating, i.e. Rayleigh-Bénard convection (RBC), proving results for IHC is more difficult, with no known rigorous results for IHC subject to rotation.

The influence of rotation alters turbulent convection and introduces new flow regimes and physics (see Ecke & Shishkina (2023) for a recent review). The flow features of rotating convection in a plane layer are well-established for boundary heating (Chandrasekhar 1961; Veronis 1959; Rossby 1969; Boubnov & Golitsyn 2012; Julien *et al.* 1996; Knobloch 1998; Vorobieff & Ecke 2002; Stevens *et al.* 2013), and some insight exists for non-uniform IHC (Barker *et al.* 2014; Currie *et al.* 2020; Hadjerci *et al.* 2024). However, no study has explored the flow in rotating uniform IHC. We know that rotation inhibits the onset of convective motion and stabilises the fluid, causing a bias in motion parallel to the axis of rotation and creating an Ekman boundary layer that enhances the mean vertical heat transport by Ekman pumping (Greenspan 1968). With sufficient thermal forcing, the  $E - R$  parameter space contains two extreme flow states: if  $R$  is sufficiently larger than  $E^{-1}$ , then buoyancy dominates and rotation plays little effect on the dynamics, whereas if  $E^{-1}$  is large relative to  $R$ , and the vertical velocity is nonzero, geostrophic turbulence occurs (Julien *et al.* 1996; Sprague *et al.* 2006). A wide range of flow features occur in rotating convection including, cellular flows, Taylor columns, large-scale vortices and plume-dominated convection (Grooms *et al.* 2010; Julien *et al.* 2012; Stellmach *et al.* 2014; Guzmán *et al.* 2020; Aurnou *et al.* 2020; Song *et al.* 2024).

In addition to numerous experimental and numerical studies on rotating RBC, there exist several proofs of bounds on the enhancement of heat transport due to convection, quantified with the Nusselt number,  $Nu$ , with the background field method (Constantin *et al.* 1999; Doering & Constantin 2001; Constantin *et al.* 2001; Yan 2004; Grooms & Whitehead 2014; Pachev *et al.* 2020). First introduced in the 1990s, the background field method provides a tool for proving bounds on the long-time averages of turbulence (Fantuzzi *et al.* 2022). In its original formulation, the idea involves decomposing the flow variables into a fluctuating and background component satisfying the boundary conditions to construct a variational problem for bounding the turbulent dissipation. A bound is obtained by solving the variational problem by choosing an appropriate background field and using elementary integral estimates. The method has been successfully used for many fluid flows, none more so than turbulent convection (Nobili 2023). Recent insight has shown that the background method fits within the framework of the *auxiliary functional method* (Chernyshenko *et al.* 2014; Chernyshenko 2022), which can yield sharp bounds for well-posed ODEs and PDEs under technical conditions (Tobasco *et al.* 2018; Rosa & Temam 2022).

A fundamental feature of the background field method is to take energy balances of the governing equations. However, energy identities fail to capture the effects of rotation. Note that this is not the case for a fluid driven by rotating boundaries, like in Taylor-Couette flow (Constantin 1994; Ding & Marensi 2019; Kumar 2022). For convection subject to the Coriolis force, standard applications of the background field method do not give a bound on  $Nu$  that includes  $E$ . One path for progress is in the limit of infinite  $Pr$ , where the momentum equation simplifies to a forced Stokes flow, leading to a diagnostic equation between the velocity and temperature, facilitating better estimates. Notably, without rotation ( $E = \infty$ ), using the background method, it was proven, up to constants and logarithms, that  $Nu \leq Ra^{1/3}$  (Doering *et al.* 2006), where  $Ra$  is the temperature difference based Rayleigh number, improving on the bound of  $Nu \leq Ra^{1/2}$  valid at arbitrary  $Pr$  (Doering & Constantin 1996). Under rotation ( $E < \infty$ ) at  $Pr = \infty$ , established results for RBC are illustrated in fig. 2.

Typically, high  $Pr$  is an undesired restriction on the parameter space when modelling fluid flows, but proving bounds in the limit of  $Pr = \infty$  can be seen as a first step towards establishing bounds valid for all  $Pr$ . Recent studies suggest that for any bound proven at infinite  $Pr$  in RBC, a semi-analytic bound for finite  $Pr$  can be obtained under specific conditions (Tilgner 2022). The results demonstrate that the bounds for finite  $Pr$  are, to highest order, equivalent to the infinite  $Pr$  results, with smaller  $R$ ,  $Pr$  and  $E$  corrections. The result is unsurprising since bounds at infinite  $Pr$  are generally improvements over those obtained for finite  $Pr$ , and can be understood as a consequence of the mathematical closeness of the turbulent attractors of both systems (Wang 2007).

When rotation dominates over buoyancy, in RBC heuristic arguments suggest that  $Nu \sim E^{3/2} Ra^2$ , at arbitrary  $Pr$  (King *et al.* 2013; Plumley & Julien 2019; Aurnou *et al.* 2020). Bounds that scale similarly to the physical arguments in the rapidly rotating regime can be proven when working with an asymptotic approximation of the governing equations known as the non-hydrostatic quasigeostrophic (nhQG) equations (Julien *et al.* 1996, 2016). Scaling the horizontal length scales by  $E^{1/3}$  and adjusting the time variable yields the nhQG equations that model the limit of rapidly rotating convection in a plane layer. Applying the background method to the nhQG equations gives the green bounds in fig. 2 and are, up to constants,  $Nu \leq E^2 Ra^2$ , for no-slip conditions (Pachev *et al.* 2020).

IHC remains less studied in part due to significant differences in the physics between RBC. Notably, in uniform IHC between isothermal boundaries, the mean conductive heat flux is zero, rendering the standard definition of the Nusselt number inapplicable (Goluskin 2016). In previous works with zero rotation (Goluskin 2016), an alternative measure of

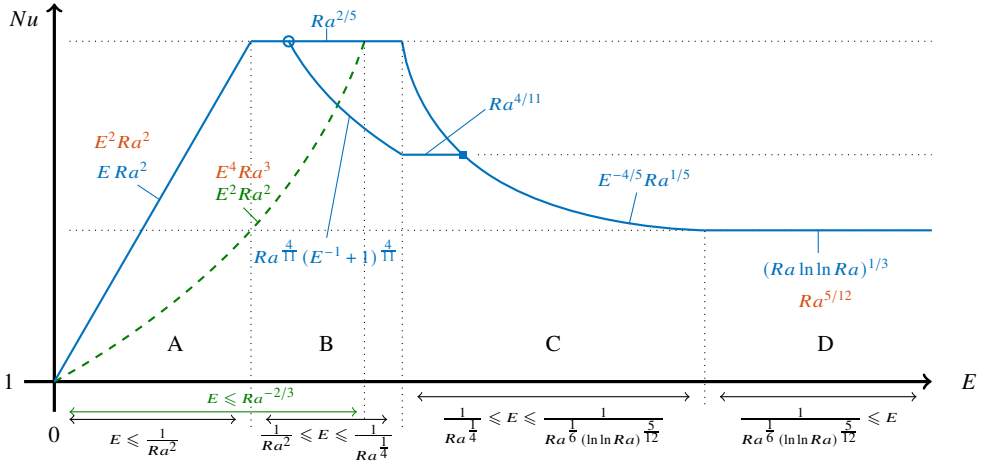


Figure 2: Illustration of the upper bounds with blue lines (—) on the Nusselt number,  $Nu$ , in terms of the Rayleigh,  $Ra$ , and Ekman numbers,  $E$ , for infinite Prandtl number rotating Rayleigh-Bénard convection, between no-slip boundaries. All bounds hold up to constants that determine the exact sizes of the regions, with red text to show the stress-free result in the same region. The bounds in A are due to Constantin *et al.* (1999). The green dashed line (---) crossing A and B show the upper bound obtained from the non-hydrostatic quasigeostrophic approximation (Pachev *et al.* 2020; Grooms & Whitehead 2014). In B, the crossover from the bound  $Ra^{2/5}$  (Doering & Constantin 2001) to  $Ra^{4/11}(E^{-1} + 1)^{4/11}$  (Yan 2004), shown by a blue circle (○), is given by the values of the constants of both bounds. The same holds for C with the crossover from  $Ra^{4/11}$  (Yan 2004) to  $E^{-4/5}Ra^{1/5}$  (Constantin *et al.* 2001) shown by a blue square (■). Region D shows the bounds for buoyancy-driven convection (Otto & Seis 2011; Whitehead & Doering 2011*b*). The transition from C to D is continuous up to logarithmic corrections (Constantin *et al.* 1999).

the turbulent convection is the mean temperature,  $\overline{\langle T \rangle}$ , where angled brackets  $\langle \cdot \rangle$  denote a volume and overbars a long-time average. As the flow becomes increasingly turbulent, the temperature within the domain becomes homogenised, quantified in a lower value of  $\overline{\langle T \rangle}$ , and a higher proxy Nusselt number defined as  $Nu_p = 1/\overline{\langle T \rangle}$ . An additional measure of turbulence is  $\overline{\langle wT \rangle}$ , quantifying the portion of heat leaving through each boundary,  $\mathcal{F}_T$  and  $\mathcal{F}_B$ , due to the effect of convection (Goluskin & Spiegel 2012). For a stationary fluid, the heat supplied leaves the domain symmetrically out of both boundaries to ensure the statistical stationarity of the solutions. As the thermal forcing increases, convection carries heat upwards, causing a higher portion of the heat to leave through the top relative to the bottom boundary (Goluskin & van der Poel 2016).

In line with previous works on uniform internally heated convection (Goluskin 2016; Arslan *et al.* 2021*a,b*; Kumar *et al.* 2022; Arslan *et al.* 2023; Arslan & Rojas 2024), the non-dimensional heat flux out of the top and bottom boundaries is given by

$$\mathcal{F}_T := -\overline{\langle \partial_z T \rangle}_h|_{z=1} = \frac{1}{2} + \overline{\langle wT \rangle} \quad \text{and} \quad (1.1a)$$

$$\mathcal{F}_B := \overline{\langle \partial_z T \rangle}_h|_{z=0} = \frac{1}{2} - \overline{\langle wT \rangle}. \quad (1.1b)$$

The non-dimensionalisation sets the limits of  $\overline{\langle wT \rangle}$  as 0 and  $\frac{1}{2}$ , with each limit corresponding to no convection and infinitely effective convection, respectively. We seek bounds of the form,  $\mathcal{F}_B \geq f_1(R, E)$  and  $\overline{\langle T \rangle} \geq f_2(R, E)$ , where  $f_1$  and  $f_2$  are functions of  $R$  and  $E$  to be determined for the emergent quantities of the flow, in different regimes of  $E - R$

space. In previous applications of the background field method to IHC, bounds for  $\overline{\langle T \rangle}$  are proven with minor adaptation from the background method as applied to RBC (Lu *et al.* 2004; Whitehead & Doering 2011a, 2012). However, in the case of obtaining bounds on  $\overline{\langle wT \rangle}$  and consequently  $\mathcal{F}_B$ , it has been established that the variational problem requires a minimum principle on  $T$ , which states that temperature in the domain is greater than or equal to zero (Arslan *et al.* 2021b). The minimum principle is necessary to obtain lower bounds on  $\mathcal{F}_B$  that remain positive as  $R$  increases. In the case of no rotation at  $Pr = \infty$ , the best-known lower bound on the mean temperature, up to constants, are  $\overline{\langle T \rangle} \geq (R \ln R)^{-1/4}$  (Whitehead & Doering 2011a) and  $\overline{\langle T \rangle} \geq R^{-5/17}$  (Whitehead & Doering 2012) for no-slip and stress-free boundaries. Conversely, the best-known lower bounds on the heat flux out of the domain are  $\mathcal{F}_B \geq R^{-2/3} + R^{-1/2} |\ln(1 - R^{-1/3})|$  and  $\mathcal{F}_B \geq R^{-40/29} + R^{-35/29} |\ln(1 - R^{-10/29})|$  (Arslan & Rojas 2024) for the two different kinematic boundary conditions.

In this paper, we prove that for uniform internally heated convection subject to rotation at an infinite Prandtl number that,

$$\mathcal{F}_B \gtrsim \begin{cases} R^{-1} + R^{-4/5} |\ln(1 - R^{-2/5})|, & E \leq R^{-2}, \\ R^{-2/3} E^{2/3} + R^{-1/2} E^{1/2} |\ln(1 - R^{-1/3} E^{1/3})|, & E \leq E_0, \\ R^{-2/3} + R^{-1/2} |\ln(1 - R^{-1/3})|, & E_0 \leq E \leq E_m, \end{cases} \quad (1.2)$$

and

$$\overline{\langle T \rangle} \gtrsim \begin{cases} R^{-1/3}, & E \leq R^{-2/3}, \\ R^{-1} E^{-1}, & E \geq R^{-2/3}, \\ R^{-2/7} E^{2/7}, & E \leq E_1, \\ R^{-2/7}, & E_1 \leq E \leq E_m, \end{cases} \quad (1.3)$$

where  $\gtrsim$  denotes that the bounds hold up to constants determined in subsequent sections and  $E_0$ ,  $E_1$  and  $E_m$  are positive constants determining the regimes of validity in  $E - R$  space of each bound. For notation,  $\|f\|_p^p = \int_0^1 f^p dz$ , for  $p < \infty$  and  $\|f\|_\infty = \text{ess sup}_{z \in [0,1]} f$  for  $p = \infty$ , represents the standard  $L^p$  norm of  $f : [0, 1] \rightarrow \mathbb{R}$ . The paper is structured as follows. In section 2, we describe the problem setup before discussing the onset of convection in section 3. Then section 4 proposes heuristic scaling arguments for rotating IHC, before we prove bounds on  $\mathcal{F}_B$  in section 5 and on  $\overline{\langle T \rangle}$  in section 6. Finally, section 7 offers a brief discussion and concluding remarks.

## 2. Setup

We consider a layer of fluid in a rotating frame of reference between two horizontal plates separated by a distance  $d$  and periodic in the horizontal ( $x$  and  $y$ ) directions with periods  $L_x d$  and  $L_y d$ . The fluid has kinematic viscosity  $\nu$ , thermal diffusivity  $\kappa$ , density  $\rho$ , specific heat capacity  $c_p$  and thermal expansion coefficient  $\alpha$ . Gravity acts in the negative vertical direction with strength  $g$ , the fluid rotates at rate  $\Omega$  and is uniformly heated internally at a volumetric rate  $H$ .

To non-dimensionalise the problem, we use  $d$  as the characteristic length scale,  $d^2/\kappa$  as the time scale and  $d^2 H/\kappa \rho c_p$  as the temperature scale (Roberts 1967). The velocity of the fluid  $\mathbf{u}(\mathbf{x}, t) = u(\mathbf{x}, t)\mathbf{e}_1 + v(\mathbf{x}, t)\mathbf{e}_2 + w(\mathbf{x}, t)\mathbf{e}_3$  and temperature  $T(\mathbf{x}, t)$  in the non-dimensional domain  $V = [0, L_x] \times [0, L_y] \times [0, 1]$  are governed by the infinite Prandtl number Boussinesq

equations,

$$\nabla \cdot \mathbf{u} = 0, \quad (2.1a)$$

$$\nabla p + E^{-1} \mathbf{e}_3 \times \mathbf{u} = \nabla^2 \mathbf{u} + R T \mathbf{e}_3, \quad (2.1b)$$

$$\partial_t T + \mathbf{u} \cdot \nabla T = \nabla^2 T + 1. \quad (2.1c)$$

The non-dimensional numbers are the Ekman and Rayleigh numbers, defined as

$$E = \frac{\nu}{2\Omega d^2}, \quad \text{and} \quad R = \frac{g\alpha H d^5}{\rho c_p \nu \kappa^2}. \quad (2.2)$$

The boundary conditions are of no-slip and isothermal temperature, respectively:

$$\mathbf{u}|_{z=\{0,1\}} = 0, \quad (2.3a)$$

$$T|_{z=\{0,1\}} = 0. \quad (2.3b)$$

Figure 1 provides a schematic for the system under consideration. The vertical component of the curl and double curl of (2.1b) gives a diagnostic equation involving the vertical velocity  $w$ , the vertical vorticity  $\zeta$  and temperature  $T$ :

$$\nabla^4 w = E^{-1} \partial_z \zeta - R \Delta_h T, \quad (2.4a)$$

$$\nabla^2 \zeta = -E^{-1} \partial_z w, \quad (2.4b)$$

where  $\Delta_h = \partial_x^2 + \partial_y^2$  is the horizontal Laplacian.

The final ingredients are results from Yan (2004) and Constantin *et al.* (1999) and a minimum principle on  $T$ . We state the results as separate lemmas.

LEMMA 1 (MINIMUM PRINCIPLE). *Suppose  $T(\mathbf{x}, t)$  solves the heat equation (2.1c) subject to (2.3b) where  $\mathbf{u}$  satisfies  $\nabla \cdot \mathbf{u} = 0$  and (2.3a). Let the negative parts of  $T(\mathbf{x}, t)$  be*

$$T_-(\mathbf{x}, t) := \max\{-T(\mathbf{x}, t), 0\}. \quad (2.5)$$

Then

$$\langle |T_-(\mathbf{x}, t)|^2 \rangle \leq \langle |T_-(\mathbf{x}, 0)|^2 \rangle \exp(-\mu t), \quad (2.6)$$

for some  $\mu > 0$ . In particular, if  $T(\mathbf{x}, 0) > 0$ , then  $T_-(\mathbf{x}, 0) = 0$  and  $T(\mathbf{x}, t) \geq 0 \forall t$ .

See the appendix A of Arslan *et al.* (2021b) for a proof.

LEMMA 2 (YAN (2004)). *Let  $w_{\mathbf{k}}, T_{\mathbf{k}} : (0, 1) \rightarrow \mathbb{R}$ , functions satisfying (2.4),  $\nabla \cdot \mathbf{u} = 0$ , subject to the velocity boundary conditions (2.3a). Then,*

- For  $\mathbf{k} \leq 1$

$$\|w_{\mathbf{k}}''\|_{\infty} \leq c_1 R (1 + \frac{1}{4} E^{-2})^{1/4} \|T_{\mathbf{k}}\|_2, \quad (2.7)$$

where  $c_1 = 6^{1/4}$ .

- For  $\mathbf{k} \geq 1$

$$\|w_{\mathbf{k}}''\|_{\infty} \leq c_2 R \sqrt{\mathbf{k}} \|T_{\mathbf{k}}\|_2 + c_2 R E^{-1} \|T_{\mathbf{k}}\|_2, \quad (2.8)$$

where  $c_2 = 1 + \frac{e^2+1}{e^2-1} \frac{4 \cosh 1 + 2 \sinh 1}{-1 + \sinh 1} \sim 64.8734$ .

LEMMA 3 (CONSTANTIN *ET AL.* (1999)). *Let  $w, T : V \rightarrow \mathbb{R}$  be horizontally periodic functions such that they solve (2.4) subject to  $\nabla \cdot \mathbf{u} = 0$  and the boundary conditions (2.3a), then*

$$\langle |\nabla^2 w|^2 \rangle + 2 \langle |\nabla \zeta|^2 \rangle \leq R^2 \langle |T|^2 \rangle. \quad (2.9)$$

### 3. Onset of convection

Before proving bounds on the emergent properties of the turbulence ( $\mathcal{F}_B$  and  $\overline{\langle T \rangle}$ ), we briefly discuss the onset of convection for (2.1). The trivial solution of (2.1) is found by taking  $\mathbf{u} = 0$  and considering a steady state where the temperature is independent of time. The conductive temperature profile,

$$T_c = \frac{1}{2}z(1 - z), \quad (3.1)$$

represents the transport of heat by conduction alone. In the case where there is no rotation ( $E = \infty$ ) for the boundary conditions in (2.3), the system becomes linearly unstable for all  $R > 37\,325.2$  (Goluskin 2016). However, unlike Rayleigh-Bénard convection when considering (2.1) in the form

$$\frac{ds}{dt} + \mathcal{L}s + \mathcal{N}(s, s) + \mathcal{P}p = 0, \quad (3.2)$$

where  $\mathcal{L}$  and  $\mathcal{P}$  are linear operators,  $\mathcal{N}$  is a bilinear operator and  $s = (\mathbf{u}, T)$  the state vector, the linear operator  $\mathcal{L}$  of (2.1) has a non-zero skew-symmetric component and nonlinear instability can occur at  $R = 26\,926.6$ , implying that subcritical convection can occur for internally heated convection (Straughan 2013; Goluskin 2016). For  $E < \infty$ , rotation stabilises the system to vertical motion and inhibits the onset of convection. For the case of RBC, the effect of rotation on the onset of convection is well quantified (Chandrasekhar 1961). In this section, we demonstrate a result for the effect of rotation on the Rayleigh number for linear instability,  $R_L$ , in IHC.

#### 3.1. Linear stability

The Rayleigh number up to which the flow is linearly stable is identified by analysing the evolution of perturbations from the linearised system of (2.1). In the non-rotating case, for selected thermal boundary conditions, the marginally stable states are stationary (Davis 1969; Herron 2003). When the flow is subject to rotation, the condition for steady rolls, as opposed to oscillatory-in-time rolls, at the onset of convection is unknown. For comparison, in the case of RBC, the onset modes are steady provided  $Pr \geq 0.68$ , such that assuming a sufficiently large  $Pr$  fluid removes the question of oscillatory motion in the analysis we carry out here. The precise structure of the motion at the onset should not affect the asymptotic behaviour of  $R_L$  for a small Ekman number. It is noteworthy that in the case of the rotating internally heated fluid sphere, the first convective modes are always unsteady (Roberts 1968; Busse 1970; Jones *et al.* 2000) and recent evidence from numerical simulations confirms the existence subcritical convection (Guervilly & Cardin 2016; Kaplan *et al.* 2017).

Taking the setup as described in section 2, we start by decomposing the temperature field into perturbations from the conductive profile  $T_c(z)$ ,

$$T(\mathbf{x}, t) = \vartheta(\mathbf{x}, t) + T_c(z), \quad (3.3)$$

to obtain the temperature perturbation,  $\vartheta$  equation from (2.1c) and boundary conditions of

$$\partial_t \vartheta + \mathbf{u} \cdot \nabla \vartheta = \nabla^2 \vartheta + T'_c w, \quad (3.4a)$$

$$\vartheta|_{z=\{0,1\}} = 0, \quad (3.4b)$$

where primes denote derivative with respect to  $z$ . Then, we look at the marginally stable stationary states of the linearised system of (2.1) by considering the  $z$  component of the double curl of the momentum equation and the vertical component of the vorticity equation;



we thus have

$$\nabla^4 w = E^{-1} \partial_z \zeta - R \nabla_H^2 \vartheta, \quad (3.5a)$$

$$\nabla^2 \zeta = -E^{-1} \partial_z w, \quad (3.5b)$$

$$\nabla^2 \vartheta = T'_c w. \quad (3.5c)$$

Given horizontal periodicity, we take a Fourier series expansion in the horizontal ( $x$  and  $y$ ) directions of the form,

$$\begin{bmatrix} \vartheta(x, y, z) \\ \mathbf{u}(x, y, z) \\ \zeta(x, y, z) \end{bmatrix} = \sum_{\mathbf{k}} \begin{bmatrix} \hat{\vartheta}_{\mathbf{k}}(z) \\ \hat{\mathbf{u}}_{\mathbf{k}}(z) \\ \hat{\zeta}_{\mathbf{k}}(z) \end{bmatrix} e^{i(k_x x + k_y y)}, \quad (3.6)$$

where the sum is over wavevectors  $\mathbf{k} = (k_x, k_y)$  with magnitude  $k = \sqrt{k_x^2 + k_y^2}$  and hats denote functions of  $z$  only. Then, substituting (3.6) into (3.5) gives

$$(D^2 - k^2)^2 \hat{w}_{\mathbf{k}} = E^{-1} \hat{\zeta}'_{\mathbf{k}} + R k^2 \hat{\vartheta}_{\mathbf{k}}, \quad (3.7a)$$

$$(D^2 - k^2) \hat{\zeta}_{\mathbf{k}} = -E^{-1} \hat{w}'_{\mathbf{k}}, \quad (3.7b)$$

$$(D^2 - k^2) \hat{\vartheta}_{\mathbf{k}} = T'_c \hat{w}_{\mathbf{k}}, \quad (3.7c)$$

where  $D^2 = \frac{d^2}{dz^2}$ . For no-slip or stress-free boundary conditions,  $\hat{\zeta}_{\mathbf{k}}$  and  $\hat{\vartheta}_{\mathbf{k}}$  can be eliminated from (3.7) to give

$$(D^2 - k^2)^3 \hat{w}_{\mathbf{k}} + E^{-2} \hat{w}''_{\mathbf{k}} = R k^2 T'_c \hat{w}_{\mathbf{k}}. \quad (3.8)$$

Here, (3.8) is an eigenvalue problem and can be solved numerically by fixing  $E$  and finding the  $R$  at which the first eigenvalue changes sign. The equivalent problem for RBC is well documented (Chandrasekhar 1961), however unlike RBC, the ODE in (3.8) admits solutions which are hypergeometric functions because  $T_c$  in (3.1) is a non-constant function. As such, even in the case of stress-free boundary conditions where  $\hat{w}_{\mathbf{k}} = \hat{w}''_{\mathbf{k}} = \hat{w}''''_{\mathbf{k}} = 0$  at both boundaries, (3.8) becomes complicated to solve. Instead, we consider the asymptotic regime of small  $E$  where a simplified form of (3.8) gives the desired asymptotic relation between  $R_L$  and  $E$ . Following the argument first presented in Chandrasekhar (1961), we posit that for  $R$  close to  $R_L$ , the wavenumber  $k$  tends to infinity so that we retain only terms in  $E$ ,  $R$  and the highest power in  $k$  and (3.8) becomes

$$E^{-2} \hat{w}''_{\mathbf{k}} = k^2 (R(\frac{1}{2} - z) + k^4) \hat{w}_{\mathbf{k}}. \quad (3.9)$$

Since (3.9) is of second order, we require only two boundary conditions. However, in the simplest set of boundary conditions of stress-free boundaries where  $\hat{w}_{\mathbf{k}}$  and  $\hat{w}''_{\mathbf{k}}$  are zero, the problem is over-determined with four boundary conditions. It suffices to take  $\hat{w}_{\mathbf{k}}(0) = \hat{w}''_{\mathbf{k}}(0) = 0$ , such that we can make the ansatz that

$$\hat{w}_{\mathbf{k}} = Ai(n - mz) - \frac{Ai(n)}{Bi(n)} Bi(n - mz), \quad (3.10)$$

where  $Ai(z)$  and  $Bi(z)$  are the Airy functions of the first and second kind. Substituting (3.10) back into (3.9) gives

$$E^{-2} m^2 (n - mz) = \frac{1}{2} k^2 R + k^6 - k^2 R z, \quad (3.11)$$

from which we require the choice that  $m = (k^2 R E^2)^{\frac{1}{3}}$ . Substituting for  $m$  and rearranging,



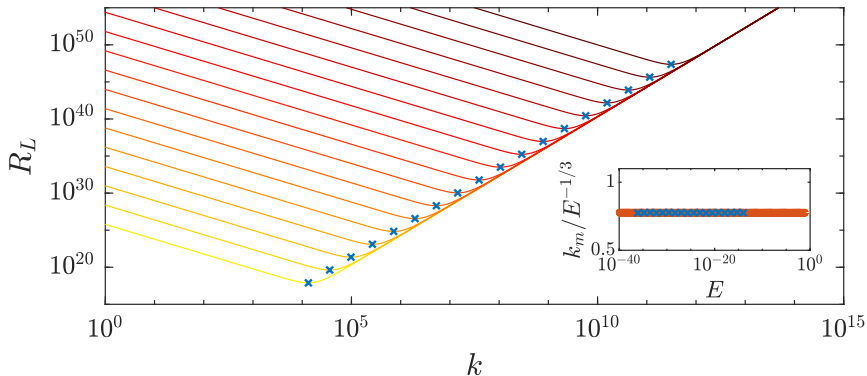


Figure 3: Plot of  $R_L$  against  $k$  as given by (3.13) for Ekman numbers ranging from  $10^{-37}$  (red) to  $10^{-13}$  (yellow). The blue dots represent the minimum  $R_L$  in  $k$ , and the inset demonstrates that the minimum wavenumber  $k_m$  varies as  $E^{-1/3}$  with a compensated plot.

we obtain

$$-\frac{1}{2}E^{2/3}k^{2/3}R + nR^{2/3} - E^{2/3}k^{14/3} = 0. \quad (3.12)$$

Given that (3.12) is a cubic equation in  $R^{1/3}$ , by application of the cubic formula, we find the real root to be,

$$R_L^{1/3} = \frac{2n}{3E^{2/3}k^{2/3}} + \frac{1}{3E^{2/3}k^{2/3}} \left( -8n^3 + 27E^2k^6 + 27E^2k^3 \sqrt{k^6 - \frac{16n^3}{27E^2}} \right)^{1/3} + \frac{4n^2}{3E^{2/3}k^{2/3}} \left( -8n^3 + 27E^2k^6 + 27E^2k^3 \sqrt{k^6 - \frac{16n^3}{27E^2}} \right)^{-1/3}. \quad (3.13)$$

Then, we want to find the smallest possible  $R_L$  in (3.13) by finding the minimising  $k$  by solving  $\partial_k R_L^{1/3} = 0$  and substituting back into (3.13) to obtain  $R_L$  as a function of only  $E$ . In fig. 3 we plot  $R_L$  from (3.13) against  $k$  for a wide range of  $E$  ( $10^{-37}$  to  $10^{-13}$ ), highlighting the minimum in  $k$  found. The inset in fig. 3 demonstrates that the  $k_m$  varies as  $E^{-1/3}$ . Given fig. 3, and noting that in the asymptotic limit of small  $E$  we assume large wavenumbers  $k$ , it is natural in (3.13) to take the minimising wavenumber to be

$$k_m^6 = \frac{16n^3}{27E^2}, \quad (3.14)$$

such that the terms in the cube roots are real and positive. Then, substituting  $k_m$  back into (3.13) and the minimal  $R_L(n, E)$  is achieved with  $n = 1$ , such that (3.13) simplifies to

$$R_L = \frac{(1 + 2^{2/3} + 2^{4/3})^3}{9 \cdot 2^{1/3}} E^{-4/3} \sim E^{-4/3}. \quad (3.15)$$

The asymptotic scaling is equivalent to rotating RBC, unsurprising given the equivalence of the momentum equations, albeit with different prefactors, and highlights the inhibiting effect of rotation on the Rayleigh number for the system to become linearly unstable. In the rest of the paper, we will use (3.15) to arrive at heuristic scaling arguments and later contextualise the bounds proven.

#### 4. Heuristics scaling arguments

Owing to the lack of data on uniform internally heated convection subject to rotation, we cannot comment on the sharpness of the bounds we will prove. Instead, we can use standard physical arguments to determine possible scaling laws for  $\overline{\langle T \rangle}$  and  $\mathcal{F}_B$ . In previous studies, the theory of Grossman & Lohse (Grossmann & Lohse 2000; Ahlers *et al.* 2009) has been adapted to uniform and exponentially varying IHC to determine scaling laws in the non-rotating case (Wang *et al.* 2020; Creyssels 2020, 2021). Here, we will follow the heuristic arguments presented in Arslan *et al.* (2021*b*) that adapt the ideas of marginal stability and diffusivity free scaling (Malkus 1954; Priestley 1954; Spiegel 1963) and combine them with arguments for rotation-dominated convection (Stevenson 1979; King *et al.* 2009; Ecke & Shishkina 2023).

The starting point is to suppose that the heat flux out of the domain, defined in (1.1), instead can be written as  $\mathcal{F}_B \sim \overline{\langle T \rangle}/\delta$  and  $\mathcal{F}_T \sim \overline{\langle T \rangle}/\varepsilon$ , remembering that energy balance gives that  $\mathcal{F}_B + \mathcal{F}_T = 1$ . In this section,  $\sim$  means approximately equal to up to constants. Then, in the buoyancy and rotation-dominated regimes, we suppose that to the highest order, the mean temperature is a function of the Rayleigh and Ekman numbers, more precisely

$$\overline{\langle T \rangle} \sim R^{-\alpha}, \quad \text{and} \quad \overline{\langle T \rangle} \sim (R/R_L)^{-\gamma} = R^{-\gamma} E^{-4\gamma/3}, \quad (4.1)$$

where  $\alpha \in \mathbb{R}_+$  and  $\gamma \in \mathbb{R}_+$  are exponents to be determined and we have substituted for  $R_L$  with (3.15). The two main regimes of turbulent convection can be interpolated by varying the Rayleigh and Ekman numbers. However, going from buoyancy to rotation-dominated heat transport, the thermal boundary layer  $\delta$  will become larger than the Ekman boundary layer  $\delta_E$ . Note that for IHC, the thermal boundary layers at the boundaries are assumed to be of different widths. Further, assuming the internal heating balances the diffusion in the boundary layer, dimensional arguments give that  $\delta \sim \varepsilon^{1/2} \sim \overline{\langle T \rangle}^{1/2}$ , implying that  $\mathcal{F}_B \sim \overline{\langle T \rangle}^{-1/2}$ . Whereas for the Ekman boundary layers by standard arguments  $\delta_E \sim E^{1/2}$  (Stevenson 1979). Therefore, using (4.1) and supposing  $\delta \sim \delta_E$  gives

$$\gamma = \frac{3\alpha}{3 - 4\alpha}. \quad (4.2)$$

The relationship in (4.2) gives a wide range of possible scaling behaviours for the IHC as the flow transitions from buoyancy to rotation-dominated, and it then remains to determine  $\alpha$ . If we first rearrange (4.2) in terms of  $\alpha$ , then we find that  $\alpha = 3\gamma/(3 + 4\gamma)$ , meaning that if we consider  $\gamma \rightarrow \infty$ , then  $\alpha \rightarrow \frac{3}{4}$ , implying that the maximal exponent of  $\alpha$  is  $\frac{3}{4}$ , though as we will see this does not correspond to any physical arguments and is ruled out by rigorous bounds (Lu *et al.* 2004; Whitehead & Doering 2011*a*).

It remains to determine  $\alpha$  to obtain the desired heuristic scaling laws. If we use the argument of marginal stability (Malkus 1954; Howard 1963) to the unstably stratified upper thermal boundary layer,  $\varepsilon$ , we find that  $\alpha = \frac{1}{4}$ . If, instead, turbulent heat transport is independent of the fluid diffusivities and is given by a characteristic free-fall velocity (Spiegel 1963), we find  $\alpha = \frac{1}{3}$ . See Arslan *et al.* (2021*b*) for a detailed explanation of the exponents for IHC in the non-rotating case. Then, for  $\alpha = \frac{1}{4}$  or  $\frac{1}{3}$ , using (4.2) gives the following predictions in the

buoyancy and rotation-dominated regimes,

$$\text{non-rotating : } \quad \overline{\langle T \rangle} \sim \begin{cases} R^{-1/4}, & \text{classical,} \\ R^{-1/3}, & \text{ultimate,} \end{cases} \quad (4.3a)$$

$$\text{rotating : } \quad \overline{\langle T \rangle} \sim \begin{cases} R^{-3/8} E^{-1/2}, & \text{classical,} \\ R^{-3/5} E^{-4/5}, & \text{ultimate,} \end{cases} \quad (4.3b)$$

and

$$\text{non-rotating : } \quad \mathcal{F}_B \sim \begin{cases} R^{-1/8}, & \text{classical,} \\ R^{-1/6}, & \text{ultimate,} \end{cases} \quad (4.4a)$$

$$\text{rotating : } \quad \mathcal{F}_B \sim \begin{cases} R^{-3/16} E^{-1/4}, & \text{classical,} \\ R^{-3/10} E^{-2/5}, & \text{ultimate.} \end{cases} \quad (4.4b)$$

While the classical regime for a rotating flow is not physically relevant, it appears in (4.3b) and (4.4b) for completeness.

As mentioned in the introduction, one can define a proxy Nusselt number as  $Nu_p = 1/\overline{\langle T \rangle}$ . Furthermore, the temperature difference based Rayleigh number  $Ra$  is related to the flux-based Rayleigh number  $R$  through the relation that  $Nu_p = R/Ra$ . Therefore, substituting for  $R$  in the scaling laws (4.3a) and (4.3b) returns the known scaling laws for the Nusselt number in RBC of  $Nu \sim Ra^{1/2}$  and  $Nu \sim Ra^{3/2} E^2$  for the ultimate scaling. We comment on the heuristic scaling laws in section 7 and compare them to the bounds we prove in the subsequent sections.

## 5. Bounds on the heat flux out of the domain

In this section, we present proofs of the bounds in (1.2) on  $\mathcal{F}_B$  as defined by (1.1). To obtain a lower bound on  $\mathcal{F}_B$ , we prove upper bounds on  $\langle wT \rangle$  by the background method in the framework of auxiliary functionals (Arslan *et al.* 2023). First, in section 5.1, we derive the variational problem for finding  $U$  where  $\langle wT \rangle \leq U$ . In section 5.2, we outline the preliminary choices that are made for the proofs and in section 5.3, estimate the upper bound on  $\langle wT \rangle$ . Then, we first prove a bound on  $\langle wT \rangle$  valid for large Ekman numbers  $E$  in section 5.4 by the use of lemma 2, followed by a proof valid for small  $E$  in section 5.5 by using lemma 3. To provide an overview, fig. 4 illustrates the lower bounds on  $\mathcal{F}_B$ , omitting the logarithmic corrections for brevity.

### 5.1. The auxiliary functional method

Here, we outline the main steps in constructing the variational problem to obtain an upper bound on  $\langle wT \rangle$ . See previous works for a detailed derivation (Arslan *et al.* 2021b, 2023). To prove an upper bound on  $\langle wT \rangle$ , we employ the auxiliary function method (Chernyshenko *et al.* 2014; Fantuzzi *et al.* 2022). The method relies on the observation that the time derivative of any bounded and differentiable functional  $\mathcal{V}\{T(t)\}$  along solutions of the Boussinesq equations (2.1) averages to zero over infinite time, so that

$$\overline{\langle wT \rangle} = \langle wT \rangle + \frac{d}{dt} \overline{\mathcal{V}\{T(t)\}}. \quad (5.1)$$

Two key simplifications follow. The first is that we can estimate (5.1) by the pointwise-in-time maximum along the solutions of the governing equations, and this value is estimated by the maximum it can take over *all* velocity and temperature fields that are periodic in  $x$

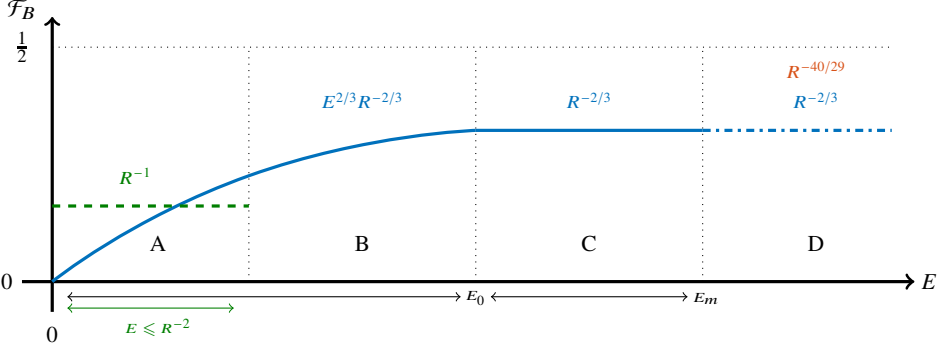


Figure 4: Illustrations of the lower bounds on the flux out of the bottom boundary,  $\mathcal{F}_B$ , between no-slip and isothermal boundary conditions at infinite  $Pr$ , the logarithmic corrections in the bounds, eq. (1.2), are suppressed for brevity. The blue plot (—) is the bound derived in section 5.4, valid up to  $E = E_m \sim 41.4487$  and  $E_0 = 4.1688$ . The bound derived in section 5.5 is shown with a green line (---). The dashed horizontal line denotes when all heat transport is by conduction and  $\mathcal{F}_B = \frac{1}{2}$ . In D (---), we show the bounds for stress-free (top, red) and no-slip (bottom, blue) at zero rotation (Arslan & Rojas 2024).

and  $y$ , satisfying incompressibility (2.1a), the boundary conditions (2.3) and the maximum principle lemma 1.

We restrict our attention to quadratic functionals taking the form

$$\mathcal{V}\{T\} := \left\langle \frac{\beta}{2} |T|^2 - [\tau(z) + z - 1]T \right\rangle, \quad (5.2)$$

that are parametrised by a positive constant  $\beta > 0$ , referred to as the balance parameter and a piecewise-differentiable function  $\tau : [0, 1] \rightarrow \mathbb{R}$  with a square-integrable derivative that we call the background temperature field. Here  $\tau(z)$  satisfies

$$\tau(0) = 1, \quad \tau(1) = 0. \quad (5.3)$$

Introducing a constant,  $U$ , and rearranging, (5.1) can be written as,

$$\overline{\langle wT \rangle} \leq U - U + \langle wT \rangle + \frac{d}{dt} \mathcal{V}\{T\} \leq U, \quad (5.4)$$

where the final inequality holds given that,  $U - \langle wT \rangle - \frac{d}{dt} \mathcal{V}\{T\} \geq 0$ , where we can substitute for the Lie derivative of  $\mathcal{V}\{T\}$  by using (2.1c). However, the minimum principle, lemma 1, is necessary to obtain a  $R$ -dependent bound on  $\overline{\langle wT \rangle}$  that approaches  $\frac{1}{2}$  from below as  $R$  increases. The condition is enforced with a Lagrange multiplier,  $\lambda(z)$ , so that the problem statement after computations as outlined in previous work (Arslan et al. 2021b, 2023) becomes

$$\overline{\langle wT \rangle} \leq \inf_{U, \beta, \tau(z), \lambda(z)} \{U \mid \mathcal{S}\{\mathbf{u}, T\} \geq 0 \quad \forall (\mathbf{u}, T) \in \mathcal{H}_+\}, \quad (5.5)$$

where

$$\mathcal{H}_+ = \{(\mathbf{u}, T) \mid \text{horizontally periodic, } \nabla \cdot \mathbf{u} = 0, (2.3), (2.4), T(\mathbf{x}) \geq 0 \text{ a.e. } \mathbf{x} \in V\},$$

provided  $\lambda(z)$  is a non-decreasing function, and

$$\mathcal{S}\{\mathbf{u}, T\} := \langle \beta |\nabla T|^2 + \tau'(z)wT + (\beta z - \tau'(z) + \lambda(z))\partial_z T + \tau(z) + U \rangle - \frac{1}{2}. \quad (5.6)$$

Ensuring the positivity of the quadratic terms in (5.6) is referred to as the *spectral constraint*

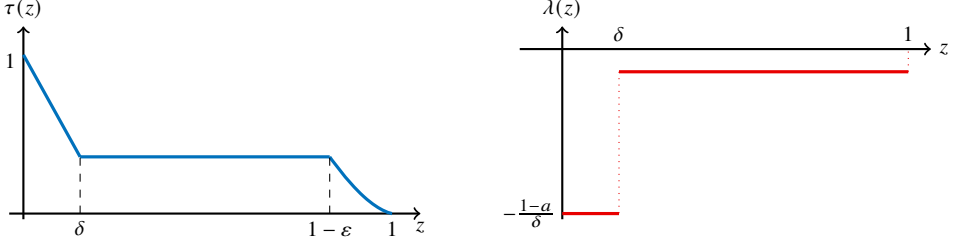


Figure 5: Sketches of the functions  $\tau(z)$  in (5.9) and  $\lambda(z)$  in (5.10) used to prove (1.2), where  $\delta$  is the boundary layer width at the bottom,  $\varepsilon$  the boundary layer width at the top of the domain and  $a$  is eq. (5.11).

and is defined as

$$\langle \beta |\nabla T|^2 + \tau'(z) w T \rangle \geq 0, \quad (5.7)$$

where  $w$  and  $T$  are related by (2.4) and subject to the boundary conditions (2.3). As has been previously established (Arslan *et al.* 2023), provided the spectral constraint is satisfied, then the non-negativity of  $\mathcal{S}\{\mathbf{u}, T\}$  is ensured when  $U$  is given by

$$\overline{\langle w T \rangle} \leq U := \frac{1}{2} + \inf_{\substack{\lambda \in L^2(0,1) \\ \lambda \text{ non decreasing} \\ \langle \lambda \rangle = -1}} \left\langle \frac{1}{4\beta} \left| \beta \left( z - \frac{1}{2} \right) - \tau'(z) + \lambda(z) \right|^2 - \tau(z) \right\rangle. \quad (5.8)$$

## 5.2. Preliminaries

To establish a bound on  $\overline{\langle w T \rangle}$ , we state the main choices used in the proof that minimise  $U(\beta, \tau, \lambda)$  as defined in (5.8). We make the following choice of background temperature field,

$$\tau(z) := \begin{cases} 1 - \frac{1-a}{\delta} z, & 0 \leq z \leq \delta, \\ a, & \delta \leq z \leq 1 - \varepsilon, \\ \frac{a(1-\varepsilon)}{\varepsilon} \left( \frac{1-z}{z} \right), & 1 - \varepsilon \leq z \leq 1, \end{cases} \quad (5.9)$$

and set  $\lambda(z)$  to be

$$\lambda(z) := \begin{cases} -\frac{1-a}{\delta}, & 0 \leq z \leq \delta, \\ -\frac{a}{1-\delta}, & \delta \leq z \leq 1. \end{cases} \quad (5.10)$$

The piecewise functions  $\tau(z)$  and  $\lambda(z)$  are quantified by the boundary layer widths  $\delta \in (0, \frac{1}{3})$  and  $\varepsilon \in (0, \frac{1}{3})$ , where  $\delta \leq \varepsilon$ , and parameter  $a > 0$  that determines the value of  $\tau(z)$  in the bulk. See fig. 5 for a sketch of the functions.

We will further fix

$$a = \frac{1}{2} \delta \varepsilon^{1/2}, \quad (5.11)$$

and

$$\beta = \frac{\langle |\tau'(z) - \lambda(z)|^2 \rangle^{1/2}}{\langle |z - \frac{1}{2}|^2 \rangle^{1/2}}. \quad (5.12)$$

In the following subsections, we prove bounds for different regimes of the Ekman number.

We achieve this by using different estimates on the spectral constraint (5.7). However, the expression for the upper bound on  $\langle wT \rangle$  in (5.8) remains the same. Therefore, first, we use our choices of  $\tau(z)$  in (5.9) and  $\lambda(z)$  in (5.10) to estimate (5.8).

### 5.3. Estimating the upper bound

Starting with (5.8) an application of the triangle inequality and the choice of  $\beta$  in (5.12) gives

$$U \leq \frac{1}{2} + \frac{1}{\sqrt{12}} \langle |\tau'(z) - \lambda(z)|^2 \rangle^{1/2} - \langle \tau \rangle. \quad (5.13)$$

Then, evaluating the sign positive integral with  $\tau(z)$  from (5.9) and  $\lambda(z)$  in (5.10), gives

$$\begin{aligned} \langle |\tau'(z) - \lambda(z)|^2 \rangle &= \int_{\delta}^1 |\tau'(z) - \lambda(z)|^2 dz \\ &= \frac{a^2}{(1-\delta)^2} (1-\varepsilon-\delta) + \frac{a^2}{\varepsilon^2} \int_{1-\varepsilon}^1 \left( \frac{1-\varepsilon}{z^2} - \frac{\varepsilon}{1-\delta} \right)^2 dz. \end{aligned} \quad (5.14)$$

We will require an upper and lower bound on (5.14). Starting with a lower bound, given that  $\varepsilon \leq \frac{1}{3}$  and  $\delta \leq \frac{1}{3}$ , with  $z$  in the range  $(1-\varepsilon, 1)$ , we make the suboptimal but simple estimate that

$$\left( \frac{1-\varepsilon}{z^2} - \frac{\varepsilon}{1-\delta} \right)^2 \geq \frac{1}{9},$$

such that we get

$$\langle |\tau'(z) - \lambda(z)|^2 \rangle \geq \frac{a^2}{\varepsilon^2} \int_{1-\varepsilon}^1 \left( \frac{1-\varepsilon}{z^2} - \frac{\varepsilon}{1-\delta} \right)^2 dz \geq \frac{a^2}{9\varepsilon}. \quad (5.15)$$

For an upper bound on (5.14), given that  $\varepsilon$  and  $\delta$  are positive, bounded above by  $\frac{1}{3}$  and that  $\delta \leq \varepsilon$ , we use the estimate  $(1-\varepsilon-\delta)(1-\delta)^{-2} \leq \frac{3}{4}\varepsilon^{-1}$  and  $z^{-2} \leq (1-\varepsilon)^{-2}$ , to obtain

$$\begin{aligned} \langle |\tau'(z) - \lambda(z)|^2 \rangle &\leq \frac{3a^2}{4\varepsilon} + \frac{a^2}{\varepsilon^2} \int_{1-\varepsilon}^1 \left( \frac{1-\varepsilon}{z^2} - \frac{\varepsilon}{1-\delta} \right)^2 dz \\ &\leq \frac{3a^2}{4\varepsilon} + \frac{a^2}{\varepsilon^2} \int_{1-\varepsilon}^1 \frac{1}{(1-\varepsilon)^2} + \frac{\varepsilon^2}{(1-\delta)^2} dz \\ &\leq \frac{3a^2}{4\varepsilon} + \frac{a^2}{\varepsilon} \frac{1+\varepsilon^2}{(1-\varepsilon)^2} \leq \frac{4a^2}{\varepsilon}. \end{aligned} \quad (5.16)$$

Moving on to the integral of  $\tau(z)$  in (5.8), we have that

$$\int_0^1 \tau(z) dz = \frac{1}{2}\delta(1-a) - \frac{a}{\varepsilon}(1-\varepsilon)\ln(1-\varepsilon). \quad (5.17)$$

Substituting (5.17) and (5.16) back into (5.13), taking  $a$  as given by (5.11) and  $\varepsilon, \delta \leq \frac{1}{3}$  such that  $\delta^2\varepsilon^{1/2} \leq \frac{\sqrt{3}}{9}\delta$ , gives

$$U \leq \frac{1}{2} - n\delta - \frac{1}{3}\delta\varepsilon^{-1/2}|\ln(1-\varepsilon)|, \quad (5.18)$$

where  $n = \frac{18-7\sqrt{3}}{36}$ .

#### 5.4. Large Ekman numbers

To obtain bounds for large  $E$  in this subsection, we will use lemma 2. The estimates in lemma 2 are pointwise estimates of the vertical velocity in Fourier space. Therefore, we exploit the horizontal periodicity of  $\mathbf{u}$  and  $T$  and take a Fourier decomposition of  $w$  and  $T$  in the spectral constraint (5.7). Taking that

$$\begin{bmatrix} T(x, y, z) \\ \mathbf{u}(x, y, z) \end{bmatrix} = \sum_{\mathbf{k}} \begin{bmatrix} T_{\mathbf{k}}(z) \\ \mathbf{u}_{\mathbf{k}}(z) \end{bmatrix} e^{i(k_x x + k_y y)}, \quad (5.19)$$

where the sum is over nonzero wavevectors  $\mathbf{k} = (k_x, k_y)$  for the horizontal periods  $L_x$  and  $L_y$  and magnitude of each wavevector is  $k = \sqrt{k_x^2 + k_y^2}$ . To lighten the notation in what follows, unlike in section 3, we do not use hats for the Fourier coefficients, even though the functions represent the same quantities. Inserting the Fourier expansions (5.19) into (5.7) give

$$\int_0^1 \beta |T'_{\mathbf{k}}|^2 + \beta k^2 |T_{\mathbf{k}}|^2 + \tau'(z) |w_{\mathbf{k}} T_{\mathbf{k}}| dz \geq 0, \quad (5.20)$$

where the complex conjugate relations of  $w_{\mathbf{k}} = w_{\mathbf{k}}^*$  holds, and  $w_{\mathbf{k}}$  and  $T_{\mathbf{k}}$  are subject to the boundary conditions

$$w_{\mathbf{k}}(0) = w_{\mathbf{k}}(1) = w'_{\mathbf{k}}(0) = w'_{\mathbf{k}}(1) = 0, \quad (5.21a)$$

$$T_{\mathbf{k}}(0) = T_{\mathbf{k}}(1) = 0. \quad (5.21b)$$

Based on the boundary conditions, we infer the following two estimates. Given (5.21a) applying the fundamental theorem of calculus and Hölders inequality gives

$$|w_{\mathbf{k}}| = \int_0^z \int_0^\sigma |\partial_\eta^2 w_{\mathbf{k}}(\eta)| d\eta d\sigma \leq \frac{1}{2} z^2 \|w''_{\mathbf{k}}\|_\infty, \quad (5.22)$$

and for  $T_{\mathbf{k}}$ , the fundamental theorem of calculus and the Cauchy-Schwarz inequality gives

$$|T_{\mathbf{k}}| = \int_0^z |\partial_\eta T_{\mathbf{k}}(\eta)| d\eta \leq \sqrt{z} \|T'_{\mathbf{k}}\|_2. \quad (5.23)$$

Next, we substitute (5.9) into the sign indefinite term in (5.20) to obtain

$$\int_0^1 \tau'(z) |w_{\mathbf{k}} T_{\mathbf{k}}| dz = -\frac{1-a}{\delta} \int_0^\delta |w_{\mathbf{k}} T_{\mathbf{k}}| dz - \frac{a(1-\varepsilon)}{\varepsilon} \int_{1-\varepsilon}^1 z^{-2} |w_{\mathbf{k}} T_{\mathbf{k}}| dz. \quad (5.24)$$

As lemma 2 contains two estimates for different regimes of  $\mathbf{k}$ , we will split the sign indefinite term in half. Then, given that  $a \leq 1$ , use of (5.22), the Cauchy-Schwarz inequality, (2.7) and (2.8) from lemma 2 gives that

$$\begin{aligned} \frac{1-a}{\delta} \int_0^\delta |w_{\mathbf{k}} T_{\mathbf{k}}| dz &\leq \frac{1}{2\delta} \int_0^\delta z^{5/2} dz \|T'_{\mathbf{k}}\|_2 \|w''_{\mathbf{k}}\|_\infty \\ &\leq \frac{\delta^{5/2}}{14} \|T'_{\mathbf{k}}\|_2 \|w''_{\mathbf{k}}\|_\infty + \frac{\delta^{5/2}}{14} \|T'_{\mathbf{k}}\|_2 \|w''_{\mathbf{k}}\|_\infty \\ &\leq \frac{c_1}{14} \delta^{5/2} R \left(1 + \frac{1}{4} E^{-2}\right)^{1/4} \|T'_{\mathbf{k}}\|_2 \|T_{\mathbf{k}}\|_2 \\ &\quad + \frac{c_2}{14} \delta^{5/2} \|T'_{\mathbf{k}}\|_2 \left( R\sqrt{k} \|T_{\mathbf{k}}\|_2 + RE^{-1} \|T_{\mathbf{k}}\|_2 \right). \end{aligned} \quad (5.25)$$

Taking the term of order  $\sqrt{k}$  in (5.25), we estimate further by noting that from (5.23) we have



a standard Poincaré inequality of

$$\|T_k\|_2 \leq \frac{1}{\sqrt{2}} \|T'_k\|_2, \quad (5.26)$$

such that the use of Youngs' inequality twice gives

$$\begin{aligned} \frac{1}{14} \delta^{5/2} R \sqrt{k} c_2 \|T'_k\|_2 \|T_k\|_2 &\leq \frac{\beta}{2} k \|T_k\|_2 \|T'_k\|_2 + \frac{c_2^2}{392\beta} \delta^5 R^2 \|T_k\|_2 \|T'_k\|_2 \\ &\leq \frac{\beta}{2} k^2 \|T_k\|_2^2 + \frac{\beta}{8} \|T'_k\|_2^2 + \frac{c_2^2}{392\sqrt{2}\beta} \delta^5 R^2 \|T'_k\|_2^2. \end{aligned} \quad (5.27)$$

Then, substituting (5.27) into (5.25), the integral at the lower boundary becomes

$$\begin{aligned} \frac{1-a}{\delta} \int_0^\delta |w_k T_k| dz &\leq \frac{\beta}{2} k^2 \|T_k\|_2^2 + \frac{\beta}{8} \|T'_k\|_2^2 + \frac{c_2^2}{392\sqrt{2}\beta} \delta^5 R^2 \|T'_k\|_2^2 \\ &\quad + \frac{c_1}{14\sqrt{2}} \delta^{5/2} R (1 + \frac{1}{4} E^{-2})^{1/4} \|T'_k\|_2^2 + \frac{c_2}{14\sqrt{2}} \delta^{5/2} R E^{-1} \|T'_k\|_2^2. \end{aligned} \quad (5.28)$$

We realise that for a sufficiently small Ekman number, the term of order  $E^{-1}$  is larger than  $(1 + E^{-2})^{1/4}$  such that if we make the estimate

$$c_1 (1 + \frac{1}{4} E^{-2})^{1/4} \leq c_2 E^{-1}, \quad (5.29)$$

we get a quadratic form in terms of  $E^2$ , that places an upper bound on  $E$  of

$$E \leq E_m = \frac{1}{2\sqrt{2}} \left( -1 + \sqrt{1 + 64(c_2^4/c_1^4)} \right)^{1/2} = 41.4487. \quad (5.30)$$

Now, (5.28) becomes,

$$\frac{1-a}{\delta} \int_0^\delta |w_k T_k| dz \leq \frac{\beta}{2} k^2 \|T_k\|_2^2 + \frac{\beta}{8} \|T'_k\|_2^2 + \frac{c_2^2}{392\sqrt{2}\beta} \delta^5 R^2 \|T'_k\|_2^2 + \frac{c_2}{7\sqrt{2}} \delta^{5/2} R E^{-1} \|T'_k\|_2^2. \quad (5.31)$$

Returning to the integral at the upper boundary in (5.24), we apply the same procedure, where (5.22) and (5.23) are instead

$$|w_k| \leq \frac{1}{2} (1-z)^2 \|w''_k\|_\infty, \quad |T_k| \leq \sqrt{1-z} \|T'_k\|_2. \quad (5.32)$$

Given  $\varepsilon \leq \frac{1}{3}$  we use that  $z^{-2} \leq (1-\varepsilon)^{-2}$  to get

$$\frac{a(1-\varepsilon)}{\varepsilon} \int_{1-\varepsilon}^1 z^{-2} |w_k T_k| dz \leq \frac{a}{\varepsilon(1-\varepsilon)} \int_{1-\varepsilon}^1 |w_k T_k| dz \leq \frac{3a}{2\varepsilon} \int_{1-\varepsilon}^1 |w_k T_k| dz. \quad (5.33)$$

By use of lemma 2, along with (5.32), (5.26), Youngs' inequality, and (5.29), we can estimate the integral at the upper boundary to obtain

$$\begin{aligned} \frac{a(1-\varepsilon)}{\varepsilon} \int_{1-\varepsilon}^1 z^{-2} |w_k T_k| dz &\leq \frac{3a}{2\varepsilon} \int_{1-\varepsilon}^1 |w_k T_k| dz \leq \frac{\beta}{2} k^2 \|T_k\|_2^2 + \frac{\beta}{8} \|T'_k\|_2^2 \\ &\quad + \frac{9c_2^2}{6272\sqrt{2}\beta} \delta^2 \varepsilon^6 R^2 \|T'_k\|_2^2 + \frac{3}{28\sqrt{2}} c_2 \delta \varepsilon^3 R E^{-1} \|T'_k\|_2^2. \end{aligned} \quad (5.34)$$

Substituting (5.31) and (5.34) back into the spectral constraint (5.20) gives

$$\left( \frac{3\beta}{4} - \frac{c_2^2}{392\sqrt{2}} \frac{\delta^5 R^2}{\beta} - \frac{c_2}{7\sqrt{2}} \delta^{5/2} R E^{-1} - \frac{3c_2}{28\sqrt{2}} \delta \varepsilon^3 R E^{-1} - \frac{9c_2^2}{6272\sqrt{2}} \frac{\delta^2 \varepsilon^6 R^2}{\beta} \right) \|T'_k\|_2^2 \geq 0. \quad (5.35)$$

The spectral condition is satisfied provided the term in the brackets of (5.35) is non-negative. Note that we have an explicit expression for  $\beta$  in (5.12), which in conjunction with the lower bound in (5.15) gives the following lower bound on  $\beta$  of

$$\beta \geq \frac{\sqrt{3}}{3} \delta. \quad (5.36)$$

After estimating  $\beta$  from below with (5.36) and making the choice

$$\delta = \left( \frac{9}{16} \right)^{1/3} \varepsilon^2, \quad (5.37)$$

the condition for the positivity of (5.35) becomes, after rearranging,

$$1 - \frac{c_2^2}{49\sqrt{2}} \delta^3 R^2 - \frac{8c_2}{7\sqrt{6}} \delta^{3/2} R E^{-1} \geq 0. \quad (5.38)$$

In (5.38), two possible choices of  $\delta = \delta(R, E)$  guarantee the non-negativity of the left-hand side. If the second negative term dominates the first, i.e.

$$\frac{c_2^2}{49\sqrt{2}} \delta^3 R^2 \leq \frac{8c_2}{7\sqrt{6}} \delta^{3/2} R E^{-1},$$

then (5.38) becomes

$$\delta \leq \left( \frac{7\sqrt{6}}{16c_2} \right)^{2/3} R^{-2/3} E^{2/3}. \quad (5.39)$$

Taking  $\delta$  as large as possible in (5.39) and substituting back into (5.38) implies that  $E \leq 8(\sqrt{2}/3)^{1/2}$ . Whereas in the opposite scenario where,

$$\frac{8c_2}{7\sqrt{6}} \delta^{3/2} R E^{-1} \leq \frac{c_2^2}{49\sqrt{2}} \delta^3 R^2,$$

then (5.38) becomes

$$\delta \leq \left( \frac{49\sqrt{2}}{2c_2^2} \right)^{1/3} R^{-2/3}, \quad (5.40)$$

which holds for  $E \geq 8(\sqrt{2}/3)^{1/2}$ . In summary, the spectral condition holds if the condition in (5.38) is satisfied and (5.38) is guaranteed when we take  $\delta$  as large as possible in (5.39) and (5.40). As a result, we have that

$$\delta = \begin{cases} \left( \frac{7\sqrt{6}}{16c_2} \right)^{2/3} R^{-2/3} E^{2/3}, & E \leq 8(\sqrt{2}/3)^{1/2}, \\ \left( \frac{49\sqrt{2}}{2c_2^2} \right)^{1/3} R^{-2/3}, & E \geq 8(\sqrt{2}/3)^{1/2}. \end{cases} \quad (5.41)$$

and by (5.37) that,

$$\varepsilon = \begin{cases} \left( \frac{7\sqrt{6}}{12c_2} \right)^{1/3} R^{-1/3} E^{1/3}, & E \leq 8(\sqrt{2}/3)^{1/2}, \\ \left( \frac{392\sqrt{2}}{9c_2^2} \right)^{1/6} R^{-1/3}, & E \geq 8(\sqrt{2}/3)^{1/2}. \end{cases} \quad (5.42)$$

Therefore, substituting (5.41) and (5.42) back into (5.18), along with the fact that  $\overline{\langle wT \rangle} \leq U$  and (1.1) to obtain

$$\mathcal{F}_B \geq \begin{cases} d_1 R^{-2/3} E^{2/3} + d_2 R^{-1/2} E^{1/2} |\ln(1 - d_3 R^{-1/3} E^{1/3})|, & E \leq 8(\sqrt{2}/3)^{1/2}, \\ d_4 R^{-2/3} + d_5 R^{-1/2} |\ln(1 - d_6 R^{-1/3})|, & 8(\sqrt{2}/3)^{1/2} \leq E \leq E_m, \end{cases} \quad (5.43)$$

where the constants  $d_1$  to  $d_6$  are collated in appendix A. Finally, in section 5.2 we chose that both boundary layer widths are in  $(0, \frac{1}{3})$ , therefore given (5.41) and (5.42) the bound obtained in (5.43) holds for all  $R \geq 0.4715$ .

### 5.5. Small Ekman numbers

Next, we demonstrate a proof of the bound on  $\mathcal{F}_B$  valid for small  $E$  in (1.2). In this regime, we use lemma 3 to demonstrate the non-negativity of the spectral constraint (5.7). The estimates used in this subsection do not require estimates in Fourier space.

Starting with the spectral constraint in (5.7), we substitute  $\tau(z)$  from (5.9) into the sign-indefinite term to obtain

$$\langle \tau'(z)wT \rangle = -\frac{1-a}{\delta} \left\langle \int_0^\delta wT dz \right\rangle_h - \frac{a}{\varepsilon} (1-\varepsilon) \left\langle \int_{1-\varepsilon}^1 wT dz \right\rangle_h. \quad (5.44)$$

We first consider the integral in (5.44) near  $z = 0$  and obtain an estimate on  $wT$ . Since we require a lower bound on the right-hand side of (5.44), we can rearrange the order of integration of the first term on the right-hand side of (5.44) and estimate the integral from above. Given the boundary conditions (2.3), use of the fundamental theorem of calculus, (2.4b) and integration by parts gives

$$\begin{aligned} \langle |wT| \rangle_h &= \left\langle \left| \int_0^z \partial_s(wT) ds \right| \right\rangle_h = \left\langle \left| \int_0^z T \partial_s w + w \partial_s T ds \right| \right\rangle_h = \left\langle \left| \int_0^z -ET \nabla^2 \zeta + w \partial_s T ds \right| \right\rangle_h \\ &= E \langle |\zeta' T| \rangle_h + \left\langle \left| \int_0^z E \nabla \zeta \nabla T + w \partial_s T ds \right| \right\rangle_h. \end{aligned} \quad (5.45)$$

Then, given the boundary condition on the velocity and temperature in (2.3), we have that

$$|w(\cdot, z)| \leq \frac{2}{3} z^{3/2} \left( \int_0^1 |w''(\cdot, z)|^2 dz \right)^{1/2}, \quad \langle T^2 \rangle_h^{1/2} \leq \sqrt{z} \langle |\nabla T|^2 \rangle_h^{1/2}, \quad (5.46)$$

use of which, along with multiple applications of the Cauchy-Schwarz inequality in (5.45), and that for any  $f \in L^2(0, 1)$  we have  $\langle |f'|^2 \rangle_h \leq \langle |\nabla f|^2 \rangle_h \leq \langle |\nabla f|^2 \rangle$ , gives

$$\begin{aligned} \langle |wT| \rangle_h &\leq E \langle |\zeta'|^2 \rangle_h^{1/2} \langle |T|^2 \rangle_h^{1/2} + E \langle |\nabla \zeta|^2 \rangle_h^{1/2} \langle |\nabla T|^2 \rangle_h^{1/2} + \frac{z^2}{3} \left\langle \int_0^z |\partial_s T|^2 ds \right\rangle_h^{1/2} \langle |w''|^2 \rangle_h^{1/2} \\ &\leq \left( (\sqrt{z} + 1) E \langle |\nabla \zeta|^2 \rangle_h^{1/2} + \frac{1}{3} z^2 \langle |\nabla^2 w|^2 \rangle_h^{1/2} \right) \langle |\nabla T|^2 \rangle_h^{1/2}. \end{aligned} \quad (5.47)$$

Next, we use lemma 3, to bound both  $\langle |\nabla \zeta|^2 \rangle$  and  $\langle |\nabla^2 w|^2 \rangle$  from above and given that  $T$  is horizontally periodic with Dirichlet boundary conditions at  $z = 0$  and  $1$  we have the standard Poincaré inequality  $\langle |T|^2 \rangle \leq (1/\pi^2) \langle |\nabla T|^2 \rangle$ , which gives

$$\langle |wT| \rangle_h \leq \left( \frac{ER}{\sqrt{2}\pi} (1 + \sqrt{z}) + \frac{1}{3\pi} z^2 R \right) \langle |\nabla T|^2 \rangle. \quad (5.48)$$

Then, substituting back into the integral at the boundary, whereby (5.11) we have  $1 - a \leq 1$ , we get that

$$\frac{1-a}{\delta} \int_0^\delta \langle |wT| \rangle_h dz \leq \left( \frac{ER}{\sqrt{2}\pi} \left( 1 + \frac{2}{3} \delta^{1/2} \right) + \frac{1}{9\pi} \delta^2 R \right) \langle |\nabla T|^2 \rangle. \quad (5.49)$$

The same estimates can be carried out at the upper boundary with  $a$  given by (5.11) and  $z$  replaced by  $1 - z$ . Then, since  $\varepsilon \leq \frac{1}{3}$  we can take  $1 - \varepsilon \leq 1$  to obtain,

$$\frac{1}{2} \delta \varepsilon^{-1/2} (1 - \varepsilon) \int_{1-\varepsilon}^1 \langle |wT| \rangle_h dz \leq \frac{\delta \varepsilon^{1/2}}{2} \left( \frac{ER}{\sqrt{2}\pi} \left( 1 + \frac{2}{3} \varepsilon^{1/2} \right) + \frac{1}{9\pi} \varepsilon^2 R \right) \langle |\nabla T|^2 \rangle. \quad (5.50)$$

Substituting (5.49) and (5.50) back into (5.44) and then into (5.7), gives after use of the lower bound on  $\beta$  from (5.36) that

$$\left( \frac{\sqrt{3}\delta}{3} - \frac{ER}{\sqrt{2}\pi} \left( 1 + \frac{2\delta^{1/2}}{3} \right) - \frac{\delta^2 R}{9\pi} - \frac{\delta \varepsilon^{1/2} ER}{\sqrt{2}\pi} \left( 1 + \frac{2\varepsilon^{1/2}}{3} \right) - \frac{\delta \varepsilon^{5/2} R}{9\pi} \right) \langle |\nabla T|^2 \rangle \geq 0. \quad (5.51)$$

Since  $\varepsilon \leq \frac{1}{3}$  and  $\delta \leq \frac{1}{3}$ , then, we will make estimates,  $1 + 2\delta^{1/2}/3 \leq \sqrt{2}\pi/3$  and  $1 + 2\varepsilon^{1/2}/3 \leq \sqrt{2}\pi/3$ , such that after rearranging the spectral constraint becomes

$$\sqrt{3}\delta - ER - \frac{\delta^2 R}{3\pi} - \delta \varepsilon^{1/2} ER - \frac{\delta \varepsilon^{5/2} R}{3\pi} \geq 0. \quad (5.52)$$

In (5.52), the first negative term does not contain an explicit  $\delta$  dependence, and so we will at the very least require that that

$$ER \leq p\delta, \quad (5.53)$$

where  $p = \sqrt{3} - \frac{3}{2}$  is chosen for algebraic simplicity. Using (5.53) and further making the choice

$$\delta = \varepsilon^{5/2}, \quad (5.54)$$

gives

$$\frac{3}{2} - \frac{2}{3\pi} \delta R - \delta^{1/5} ER \geq 0. \quad (5.55)$$

Similar to the proof of a bound for large Ekman numbers in section 5.4, we have a constraint that we consider in two regimes. If in (5.55), the second negative term dominates the first such that

$$\frac{2}{3\pi} \delta R \leq \delta^{1/5} ER,$$

then

$$\delta \leq \frac{243}{1024} E^{-5} R^{-5}, \quad (5.56)$$

however, if this  $\delta$  is to satisfy the spectral constraint then its implication on (5.53) and (5.55) need to be checked. If we take  $\delta$  to be as large as possible in (5.56), then, up to constants, we

get from (5.53) and (5.55) that

$$E \gtrsim R^{-4/5} \quad \text{and} \quad E \lesssim R^{-1},$$

which leads to a contradiction such that the initial assumption cannot be true. Assuming instead that,

$$\delta^{1/5} E R \leq \frac{2}{3\pi} \delta R,$$

gives in (5.55) that

$$\delta \leq \frac{9\pi}{8} R^{-1}. \quad (5.57)$$

Taking  $\delta$  as large as possible in (5.57), the constraints from (5.53) and (5.55) imply that,

$$E \leq \frac{9\pi}{8} (\sqrt{3} - \frac{3}{2}) R^{-2}, \quad \text{and} \quad E \leq \frac{3}{4} \left( \frac{8}{9\pi} \right)^{1/5} R^{-4/5}. \quad (5.58)$$

The first condition in (5.58), due to (5.53), is stronger for all  $R > 1$  and defines the domain of validity for the bound. Finally, substituting the largest  $\delta$  from (5.57) into (5.54) gives

$$\varepsilon = \left( \frac{9\pi}{8} \right)^{2/5} R^{-2/5}. \quad (5.59)$$

Then, taking  $\delta$  as large as possible in (5.57), (5.59), substituting into (5.18), along with the fact that  $\langle wT \rangle \leq U$  and (1.1) we get that,

$$\mathcal{F}_B \geq d_7 R^{-1} + d_8 R^{-4/5} |\ln(1 - d_9 R^{-2/5})|, \quad E \leq \frac{9\pi}{8} (\sqrt{3} - \frac{3}{2}) R^{-2}, \quad (5.60)$$

where the constants  $d_7$  to  $d_9$  are collated in appendix A. Finally, for completeness, we verify that the choice of  $\varepsilon$ ,  $\delta \in (0, \frac{1}{3})$  made in section 5.2 is not restrictive. Since  $\delta$  is smaller than  $\varepsilon$  as expressed in eq. (5.54), taking  $\delta$  as large as possible in (5.57) the bound obtained in (5.60) holds for all  $R \geq 10.6029$ .

## 6. Bounds on the mean temperature

In this section, we prove bounds on  $\overline{\langle T \rangle}$  with the auxiliary functional method by using the same strategy as in section 5.1. First, we derive a variational problem for obtaining a lower bound on  $\overline{\langle T \rangle}$ , with a different quadratic auxiliary functional to (5.2). Then, given our choice of background profile  $\varphi(z)$ , we can estimate the lower bound  $L$  on  $\overline{\langle T \rangle}$  in terms of the parameters of  $\varphi(z)$ . We then prove bounds for large and small  $E$  numbers by lemma 2 and lemma 3. The proofs in this section are algebraically lighter than the proof for a bound on  $\langle wT \rangle$ , primarily due to two reasons. The first is that the minimum principle on  $T$ , lemma 1, is not required, and the second, the balance parameters do not have a  $R$  dependence. The lower bounds we prove on  $\overline{\langle T \rangle}$ , including those already known, are illustrated in fig. 6.

### 6.1. The auxiliary functional method

By the auxiliary functional method, we obtain an explicit variational problem that we solve to obtain a bound on  $\overline{\langle T \rangle}$ . The following derivation, albeit in the language of the classic background field method approach, appears in previous papers (Whitehead & Doering 2011a, 2012). Here, we only present an outline within the auxiliary functional framework.

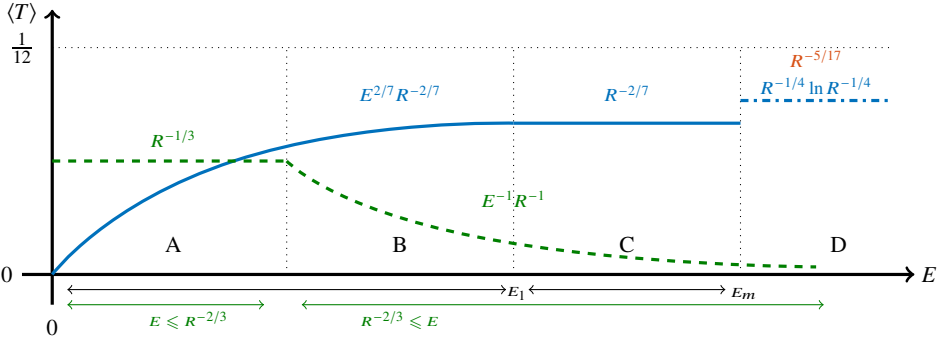


Figure 6: Illustration of the lower bounds on the mean temperature between no-slip and isothermal boundary conditions at infinite  $Pr$ . The blue plot ( $\text{—}$ ) is the bound derived in section 6.3, valid up to  $E_m \sim 41.4487$  and  $E_1 = 8$ . The bounds derived in section 6.4 are shown with a green plot ( $\text{- - -}$ ). The dashed horizontal line denotes when all heat transport is by conduction and  $\overline{\langle T \rangle} = \frac{1}{12}$ . In D ( $\text{- - -}$ ), we show the previously known best bound for stress-free (top, red) (Whitehead & Doering 2012) and no-slip (bottom, blue) (Whitehead & Doering 2011a) at zero rotation.

Starting with the quadratic auxiliary functional

$$\mathcal{V}\{T\} = \left\langle -\frac{1}{2}|T|^2 + 2\varphi(z)T \right\rangle, \quad (6.1)$$

where  $\varphi(z)$  is the background temperature field subject to the boundary conditions

$$\varphi(0) = \varphi(1) = 0. \quad (6.2)$$

Then, provided  $\mathcal{V}\{T(t)\}$  is bounded along solutions of (2.1), then the time derivative of the long-time average of  $\mathcal{V}\{T\}$  is zero, such that we can write

$$\overline{\langle T \rangle} = L - \left( L - \overline{\langle T \rangle} + \overline{\frac{d}{dt}\mathcal{V}\{T\}} \right) \geq L, \quad (6.3)$$

where the inequality comes from assuming that,  $L - \overline{\langle T \rangle} + \overline{\frac{d}{dt}\mathcal{V}\{T\}} \leq L - \overline{\langle T \rangle} - \overline{\frac{d}{dt}\mathcal{V}\{T\}} \leq 0$ . Noting that we again bound the terms in the long-time integral by the pointwise in time maximum over all periodic  $\mathbf{u}$  and  $T$ , where  $\nabla \cdot \mathbf{u} = 0$ , subject to the boundary conditions (2.3). Hence, after substituting for the Lie derivative of  $\mathcal{V}\{T\}$  by use of (2.1c) and rearranging, we have, after appropriate manipulations, the following variational problem

$$\overline{\langle T \rangle} \geq \inf_{L, \varphi(z)} \left\{ L \mid \mathcal{S}\{\mathbf{u}, T\} \geq 0 \quad \forall (\mathbf{u}, T) \in \mathcal{H}_+ \right\}, \quad (6.4)$$

where

$$\mathcal{S}\{\mathbf{u}, T\} := \langle |\nabla T|^2 + \varphi'(z)wT - \varphi'(z)\partial_z T + \varphi(z) - L \rangle. \quad (6.5)$$

In this case, the spectral constraint is given by

$$\langle |\nabla T|^2 + 2\varphi'(z)wT \rangle \geq 0. \quad (6.6)$$

Then, by optimising the linear terms in (6.5) the explicit expression for  $L$  is given

$$L := 2 \langle \varphi(z) \rangle - \langle |\varphi'(z)|^2 \rangle. \quad (6.7)$$

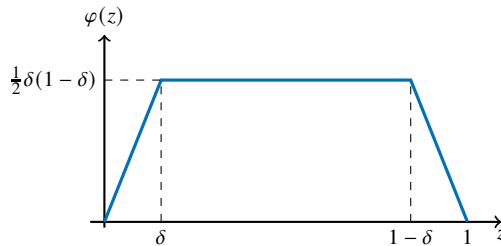


Figure 7: Sketches of the functions  $\varphi(z)$  in (6.8) used to prove (1.3), where  $\delta$  is the boundary layer widths.

### 6.2. Preliminaries

To establish a lower bound on  $\overline{\langle T \rangle}$ , we take the following class of background fields

$$\varphi(z) := \begin{cases} \frac{1}{2}(1-\delta)z, & 0 \leq z \leq \delta, \\ \frac{1}{2}\delta(1-\delta), & \delta \leq z \leq 1-\delta, \\ \frac{1}{2}(1-\delta)(1-z), & 1-\delta \leq z \leq 1. \end{cases} \quad (6.8)$$

The background field is entirely determined by  $\delta \in (0, \frac{1}{3})$ , the width of the boundary layers at the top and bottom of the domain, sketched in fig. 7. In contrast to section 5, no advantage follows from background fields with boundary layers of different widths.

The lower bounds on  $\overline{\langle T \rangle}$  for different regimes of the Ekman number rely on different estimates of the velocity in the spectral constraint (6.6) given the diagnostic equations (2.4). Given the choice of background profile (6.8), the expression for the lower bound  $L = L(\delta)$  is unchanged based on the estimates we use to demonstrate the non-negativity of the spectral constraint for different regimes of the Ekman number. So, we now estimate  $L$  in (6.7) given (6.8). Substituting for  $\varphi(z)$  from (6.8), we get

$$L = \frac{1}{2}\delta(1-\delta)^2. \quad (6.9)$$

Since  $\delta \leq \frac{1}{3}$ , then the estimate  $1-\delta \geq \frac{2}{3}$ , gives

$$L \geq \frac{2}{9}\delta. \quad (6.10)$$

### 6.3. Large Ekman numbers

We can now proceed to establish a lower bound on  $\overline{\langle T \rangle}$  by establishing the conditions under which the spectral constraint of (6.4) is satisfied, given the choice of background temperature field (6.8) and by use of lemma 2. The estimates in lemma 2 apply to (2.4) in Fourier space so we exploit horizontal periodicity and substitute (5.19) into (6.6) such that the spectral constraint in Fourier space is

$$\int_0^1 |T'_k|^2 + k^2 |T_k|^2 + 2\varphi'(z) \operatorname{Re}\{w_k T_k^*\} dz \geq 0. \quad (6.11)$$



Substituting for  $\varphi(z)$  and using the fact that  $\delta \leq \frac{1}{3}$  gives  $-(1 - \delta) \geq -1$ , the sign-indefinite of (6.11) is

$$\begin{aligned} 2 \int_0^1 \varphi'(z) \operatorname{Re}\{w_k T_k^*\} dz &\geq -2 \int_0^1 |\varphi'(z) w_k T_k| dz \\ &\geq - \int_0^\delta |w_k T_k| dz - \int_{1-\delta}^1 |w_k T_k| dz. \end{aligned} \quad (6.12)$$

Due to the symmetry in the boundary conditions and  $\varphi(z)$ , we only demonstrate estimates on the integral at the lower boundary since that at the top gives an identical contribution. Using the estimates of (5.22) and (5.23) on  $w_k$  and  $T_k$ , lemma 2 and Youngs' inequality, we get

$$\begin{aligned} \int_0^\delta |w_k T_k| dz &\leq \frac{1}{2} \int_0^\delta z^{5/2} dz \|T_k'\|_2 \|w_k''\|_\infty \\ &= \frac{1}{14} \delta^{7/2} \|T_k'\|_2 \|w_k''\|_\infty + \frac{1}{14} \delta^{7/2} \|T_k'\|_2 \|w_k''\|_\infty \\ &\leq \frac{\delta^{7/2}}{14} c_1 R (1 + \frac{1}{4} E^{-2})^{1/4} \|T_k'\|_2 \|T_k\|_2 \\ &\quad + \frac{\delta^{7/2}}{14} \|T_k'\|_2 c_2 (R\sqrt{k} \|T_k\|_2 + RE^{-1} \|T_k\|_2). \end{aligned} \quad (6.13)$$

Taking the term of order  $\sqrt{k}$ , estimating by use of Youngs' inequality twice and (5.26) gives

$$\begin{aligned} \frac{1}{14} \delta^{7/2} R\sqrt{k} c_2 \|T_k'\|_2 \|T_k\|_2 &\leq \frac{\sqrt{2}}{2} k \|T_k\|_2 \|T_k'\|_2 + \frac{c_2^2}{392\sqrt{2}} \delta^7 R^2 \|T_k\|_2 \|T_k'\|_2 \\ &\leq \frac{1}{2} k^2 \|T_k\|_2^2 + \frac{1}{4} \|T_k'\|_2^2 + \frac{c_2^2}{784} \delta^7 R^2 \|T_k'\|_2^2. \end{aligned} \quad (6.14)$$

Therefore, the integral from 0 to  $\delta$  simplifies to

$$\begin{aligned} \int_0^\delta |w_k T_k| dz &\leq \frac{1}{2} k^2 \|T_k\|_2^2 + \frac{1}{4} \|T_k'\|_2^2 + \frac{c_2^2}{784} \delta^7 R^2 \|T_k'\|_2^2 \\ &\quad + \frac{\sqrt{2}}{28} c_1 \delta^{7/2} R (1 + \frac{1}{4} E^{-2})^{1/4} \|T_k'\|_2^2 + \frac{\sqrt{2}}{28} c_2 \delta^{7/2} RE^{-1} \|T_k'\|_2^2. \end{aligned} \quad (6.15)$$

By equivalent estimates at the upper boundary, we get the same upper bound such that (6.12) becomes

$$\begin{aligned} 2 \int_0^1 \varphi'(z) \operatorname{Re}\{w_k T_k^*\} dz &\geq -k^2 \|T_k\|_2^2 - \frac{1}{2} \|T_k'\|_2^2 - \left( \frac{c_2^2}{392} \delta^7 R^2 \right. \\ &\quad \left. + \frac{\sqrt{2}}{14} c_1 \delta^{7/2} R (1 + \frac{1}{4} E^{-2})^{1/4} + \frac{\sqrt{2}}{14} c_2 \delta^{7/2} RE^{-1} \right) \|T_k'\|_2^2. \end{aligned} \quad (6.16)$$

Finally, we use the estimate in (5.29), which places an upper limit on  $E = E_m$  in (5.30), for which the bounds are valid. Then, substituting (6.16) into (6.11) with (5.29), the spectral constraint becomes

$$\frac{1}{2} - \frac{c_2^2}{392} \delta^7 R^2 - \frac{\sqrt{2}}{7} c_2 \delta^{7/2} RE^{-1} \geq 0. \quad (6.17)$$

In (6.17), two possible choices of  $\delta = \delta(R, E)$  guarantee the non-negativity of the left-hand side. If,

$$\frac{c_2^2}{392} \delta^7 R^2 \leq \frac{\sqrt{2}}{7} c_2 \delta^{7/2} R E^{-1},$$

then from we (6.17) we have that

$$\delta \leq \left( \frac{7\sqrt{2}}{8c_2} \right)^{2/7} R^{-2/7} E^{2/7}. \quad (6.18)$$

Taking (6.18) as large as possible, substituting back into (6.17) and rearranging, we find that the spectral constraint holds when  $E \leq 8$ . In the opposite scenario where,

$$\frac{\sqrt{2}}{7} c_2 \delta^{7/2} R E^{-1} \leq \frac{c_2^2}{392} \delta^7 R^2,$$

substituted back into (6.17) gives that

$$\delta \leq \left( \frac{196}{c_2^2} \right)^{1/7} R^{-2/7}, \quad (6.19)$$

which holds for  $E \geq 8$ . In summary, we have that

$$\delta = \begin{cases} \left( \frac{7\sqrt{2}}{8c_2} \right)^{2/7} R^{-2/7} E^{2/7}, & E \leq 8, \\ \left( \frac{196}{c_2^2} \right)^{1/7} R^{-2/7}, & E \geq 8, \end{cases} \quad (6.20)$$

which we can finally substitute in to (6.10) remembering that  $\overline{\langle T \rangle} \geq L$  to obtain that

$$\overline{\langle T \rangle} \geq \begin{cases} d_{10} R^{-2/7} E^{2/7}, & E \leq 8, \\ d_{11} R^{-2/7}, & 8 \leq E \leq E_m, \end{cases} \quad (6.21)$$

where  $d_{10}$  and  $d_{11}$  are in appendix A. A final check is on the validity of the bounds given choices made in section 6.2 that  $\delta$  is in  $(0, \frac{1}{3})$ . Given (6.20) the bound obtained in (6.21) holds for all  $R \geq 7.1363$  when  $E \leq 8$  and  $R \geq 10.0922$  when  $E \geq 8$ .

#### 6.4. Small Ekman numbers

Next, we move on to the proof of the lower bound on  $\overline{\langle T \rangle}$  in (1.3) valid for a small  $E$ . In this regime, we will use lemma 3, which does not require estimates in Fourier space. Starting with the spectral constraint (6.6) and substituting for  $\varphi(z)$  from (6.8), the sign-indefinite term becomes

$$2 \langle \varphi'(z) w T \rangle \geq -2 \langle |\varphi'(z) w T| \rangle \geq - \left\langle \int_0^\delta |w T| dz \right\rangle_h - \left\langle \int_{1-\delta}^1 |w T| dz \right\rangle_h. \quad (6.22)$$

In section 5.5, we established the estimate (5.48) and can directly substitute into integral at the lower boundary in (6.22) to obtain

$$\left\langle \int_0^\delta |w T| dz \right\rangle_h \leq \left[ \frac{E R}{\sqrt{2}\pi} \left( \delta + \frac{2\delta^{3/2}}{3} \right) + \frac{1}{9\pi} \delta^3 R \right] \langle |\nabla T|^2 \rangle. \quad (6.23)$$

The integral at the upper boundary gives an identical estimate such that the spectral constraint of (6.6) becomes

$$\begin{aligned} \langle |\nabla T|^2 + 2\varphi'(z)wT \rangle &\geq \langle |\nabla T|^2 - 2|\varphi'(z)wT| \rangle \\ &\geq \langle |\nabla T|^2 \rangle - 2 \left[ \frac{ER}{\sqrt{2\pi}} \left( \delta + \frac{2\delta^{3/2}}{3} \right) + \frac{1}{9\pi} \delta^3 R \right] \langle |\nabla T|^2 \rangle \geq 0. \end{aligned} \quad (6.24)$$

Therefore, the spectral constraint becomes the condition

$$1 - \frac{2ER}{\sqrt{2\pi}} \left( \delta + \frac{2\delta^{3/2}}{3} \right) - \frac{1}{9\pi} \delta^3 R \geq 0. \quad (6.25)$$

Given that  $\delta \leq \frac{1}{3}$ , we use the estimate that  $1 + 2\delta^{1/2}/3 \leq \frac{\sqrt{2\pi}}{3}$  to get the condition,

$$1 - \frac{2}{3}ER\delta - \frac{1}{9\pi}\delta^3 R \geq 0. \quad (6.26)$$

Once more, the condition admits  $\delta = \delta(R, E)$  valid for two different regimes. If we take

$$\frac{2}{3}ER\delta \leq \frac{1}{9\pi}\delta^3 R,$$

then (6.26) is non-negative if

$$\delta \leq \left( \frac{9\pi}{2} \right)^{1/3} R^{-1/3}, \quad (6.27)$$

where when taking  $\delta$  as large as possible the choice holds when  $E \leq \frac{3}{4} \left( \frac{2}{9\pi} \right)^{1/3} R^{-2/3}$ . Whereas in the case where

$$\frac{1}{9\pi}\delta^3 R \leq \frac{2}{3}ER\delta,$$

then

$$\delta \leq \frac{3}{4}R^{-1}E^{-1}, \quad (6.28)$$

for all  $E \geq \frac{3}{4} \left( \frac{2}{9\pi} \right)^{1/3} R^{-2/3}$ . Therefore, the spectral constraint is satisfied if

$$\delta = \begin{cases} \left( \frac{9\pi}{8} \right)^{1/3} R^{-1/3}, & E \leq \frac{3}{4} \left( \frac{2}{9\pi} \right)^{1/3} R^{-2/3}, \\ \frac{3}{4}R^{-1}E^{-1}, & E \geq \frac{3}{4} \left( \frac{2}{9\pi} \right)^{1/3} R^{-2/3}. \end{cases} \quad (6.29)$$

Substituting into (6.10) and remembering further that  $\overline{\langle T \rangle} \geq L$ , gives

$$\overline{\langle T \rangle} \geq \begin{cases} d_{12}R^{-1/3}, & E \leq \frac{3}{4} \left( \frac{2}{9\pi} \right)^{1/3} R^{-2/3}, \\ d_{13}R^{-1}E^{-1}, & E \geq \frac{3}{4} \left( \frac{2}{9\pi} \right)^{1/3} R^{-2/3}, \end{cases} \quad (6.30)$$

where  $d_{12}$  and  $d_{13}$  are in appendix A. Finally, for completeness, we verify that the choice of  $\delta \in (0, \frac{1}{3})$  made in section 6.2 is not restrictive. Given (6.29) the bound obtained in (6.30) holds for all  $R \geq 95.4259$  when  $E \leq \frac{3}{4} \left( \frac{2}{9\pi} \right)^{1/3} R^{-2/3}$  and for all  $R \geq 1$  otherwise.

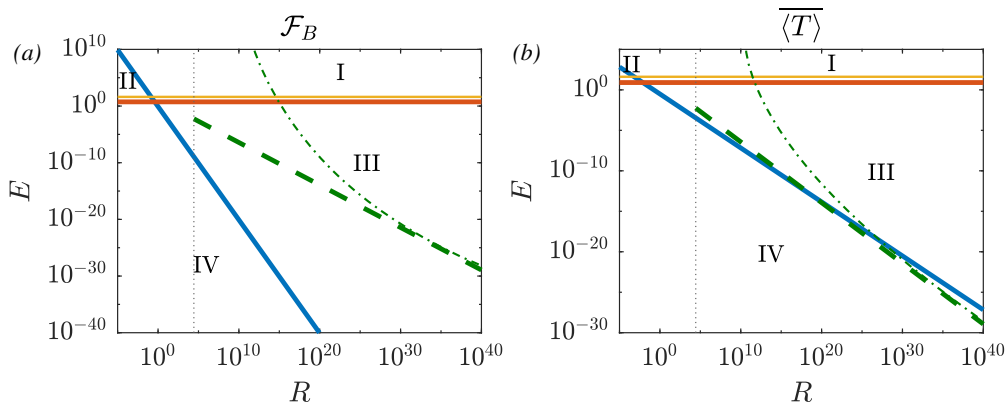


Figure 8: The Rayleigh and Ekman number regimes diagrams for the bounds (5.43), (5.60), (6.21) and (6.30). In (a), we plot the regimes for the bounds on  $\mathcal{F}_B$  and in (b) the regimes for the bounds on  $\overline{\langle T \rangle}$ . The blue solid lines (—) corresponds to  $E = 0.8201 R^{-2}$  in (a) and  $E = 0.3102 R^{-2/3}$  in (b) and the horizontal red solid lines (—) to  $E_0 = 5.4927$  in (a) and  $E_1 = 8$  in (b). In both figures, the horizontal yellow lines (—) are  $E_m = 41.4487$ , the vertical dashed lines  $R_L = 26926.6$ , the green dashed lines (---) the asymptotic result of (3.15) and the green dot dashed line (—•—) denotes the expected line above which the flow is linearly unstable for no-slip boundaries. The four main regimes are labelled I to IV.

## 7. Discussion

### 7.1. Regimes of the bounds

Owing to the use of two different estimates (lemma 2 and lemma 3), we need to consider how the bounds overlap. Furthermore, we can compare the heuristic scaling laws of (4.3a) and (4.4a), with the lower bounds (5.43), (5.60), (6.21) and (6.30). To this effect, first, we plot the regimes in which the bounds on  $\mathcal{F}_B$  and  $\overline{\langle T \rangle}$  overlap in fig. 8. For ease of understanding, we split the space of  $E$  and  $R$  into four regimes. Regime I, where  $R$  and  $E$  are large, corresponds to a slowly rotating buoyancy-dominated flow. Regime II is the solid body rotation of the fluid since  $R$  and  $E$  are small. Regime III, where  $R$  is large and  $E$  small, is rotation-dominated convection provided  $R > R_L$ , and the same applies to regime IV, where  $E$  is small and  $R$  cannot get too large. Then, we will compare the bounds to the heuristic scaling scales for rotation-dominated convection due to internal heating.

In fig. 8(a), the blue solid line shows  $E = 0.8201 R^{-2}$ , the red line is the constant  $E_0 = 5.4927$ , whereas in fig. 8(b) the blue line shows  $E = 0.3102 R^{-2/3}$ , and the red line is the constant  $E_1 = 8$ . In both (a) and (b), the yellow line is the constant  $E_m = 41.4487$  from (5.30), the dotted vertical line,  $R_L = 26926.6$  and the dashed green line is the asymptotic result of (3.15). The dot-dashed line is a sketch of the expected  $R_L$  for no-slip boundaries valid at each  $R$ , for all  $R$  below the green curves, rotation inhibits convection.

Starting with fig. 8(a), the bounds of (5.43) and (5.60) split the diagram into four and we evaluate the best bound in each regime. For regime I, where  $E \gtrsim R^{-2}$  and  $E \gtrsim E_0$ , the only valid bound is  $d_4 R^{-2/3} + d_5 R^{-1/2} |\ln(1 - d_6 R^{-1/3})|$ , however, this bound holds only up to  $E \leq E_m$ . The scaling of the slowly rotating convection bound matches the zero rotation bound of Arslan & Rojas (2024). In regime II,  $E \lesssim R^{-2}$  and  $E \gtrsim E_0$ , the best bound would match I, but the regime is below  $R_L$  when  $E = \infty$ , so no convection occurs, and  $\mathcal{F}_B = \frac{1}{2}$ . In regime III,  $E \gtrsim R^{-2}$  and  $E \leq E_0$ , the only bound is  $d_1 R^{-2/3} E^{2/3} + d_2 R^{-1/2} E^{1/2} |\ln(1 - d_3 R^{-1/3} E^{1/3})|$ , provided  $R > R_L$ . Finally, in regime IV, where  $E \lesssim R^{-2}$  and  $E \leq E_0$ , the best bound is  $d_7 R^{-1} + d_8 R^{-4/5} |\ln(1 - d_9 R^{-2/5})|$ , however for the entire region  $R < R_L$  and no convection occurs.

Table 1: Summary of the lower bounds on  $\mathcal{F}_B$  and  $\overline{\langle T \rangle}$  with respect to the regimes in fig. 8. The constants in the bounds ((5.43),(5.60),(6.21) and (6.30)) are omitted for brevity, while  $E_0 = 5.4927$  and  $E_1 = 8$ . Region I corresponds to buoyancy-dominated convection, II to no convection, III to buoyancy or rotation-dominated convection and IV to no or rotation-dominated convection.

Regime	Condition	Bound on $\mathcal{F}_B$	Condition	Bound on $\overline{\langle T \rangle}$
I	$E \gtrsim R^{-2}$ , $E \geq E_0$	$R^{-2/3} + R^{-1/2}  \ln(1 - R^{-1/3}) $	$E \lesssim R^{-2/3}$ , $E \geq E_1$	$R^{-2/7}$
II	$E \lesssim R^{-2}$ , $E \geq E_0$	$\frac{1}{2}$	$E \lesssim R^{-2/3}$ , $E \geq E_1$	$\frac{1}{12}$
III	$E \gtrsim R^{-2}$ , $E \leq E_0$	$R^{-2/3} E^{2/3} + R^{-1/2} E^{1/2}  \ln(1 - R^{-1/3} E^{1/3}) $	$E \gtrsim R^{-2/3}$ , $E \leq E_1$	$R^{-1} E^{-1}$
IV	$E \lesssim R^{-2}$ , $E \leq E_0$	$\frac{1}{2}$	$E \lesssim R^{-2/3}$ , $E \leq E_1$	$R^{-1/3}$

Moving on to fig. 8(b), which represents the bounds (6.21) and (6.30). In regime I,  $E \gtrsim R^{-2/3}$  and  $E \geq E_1$ , there are two bounds of  $d_{13}R^{-1}E^{-1}$  and  $d_{11}R^{-2/7}$ , where from a comparison of the two the better bound is  $d_{11}R^{-2/7}$ , due to the requirement of  $E \gtrsim R^{-2/3}$ . In regime II,  $E \lesssim R^{-2/3}$  and  $E \geq E_1$ , and the dominant bound would be  $d_{11}R^{-2/7}$ , but the region is below the linear stability limit, so  $\overline{\langle T \rangle} = \frac{1}{12}$ . In regime III,  $E \gtrsim R^{-2/3}$  and  $E \leq E_1$ , there are two bounds of  $d_{10}R^{-2/7}E^{2/7}$  and  $d_{13}R^{-1}E^{-1}$ , of which the second is better for all  $R > R_L$ . Remember that the dashed green line scales as  $R^{-3/4}$ , so, for sufficiently large  $R$ , the entire regime of III corresponds to convecting flows. The asymptotic result (3.15) intersects the blue line at approximately  $R = 8.569 \times 10^{18}$  and  $E = 7.407 \times 10^{-14}$ , which would be higher  $R$  and smaller  $E$ , for no-slip boundaries. In regime IV,  $E \lesssim R^{-2/3}$  and  $E \leq E_1$ , there are two bounds but the better one is  $d_{12}R^{-1/3}$ . Note that unlike for the bounds on  $\mathcal{F}_B$ , for  $\overline{\langle T \rangle}$  in regime IV, there exists a region where  $R > R_L$ , therefore for rotating convection, there are two possible scaling laws, one in regime IV and other in III of  $d_{12}R^{-1/3}$  and  $d_{13}R^{-1}E^{-1}$  respectively. Table 1 summarises the above discussion.

Finally, consider the heuristic scalings of  $\overline{\langle T \rangle} \sim R^{-3/5}E^{-4/5}$  from (4.3b) and  $\mathcal{F}_B \sim R^{-3/10}E^{-2/5}$  from (4.4b), that hold for rotation dominated convection. In both scaling laws, if we fix  $R$  and take  $E \rightarrow 0$ , we would obtain the uniform upper bounds for both quantities. The lower bounds closest to the heuristic scaling are those in region III (table 1). The bounds do not contradict the heuristic arguments and are rigorous lower bounds for future studies of rotating IHC. It is insightful to consider the small  $E$  limit where  $E \sim R_L^{-3/4}$ , and have

$$\overline{\langle T \rangle} \sim \left( \frac{R}{R_L} \right)^{-3/5}, \quad \text{and} \quad (7.1a)$$

$$\mathcal{F}_B \sim \left( \frac{R}{R_L} \right)^{-3/10}, \quad (7.1b)$$

whereas the rigorous bounds in regime III (table 1) are at best

$$\overline{\langle T \rangle} \gtrsim \left( \frac{R}{R_L} \right)^{3/14} R^{-1/2}, \quad \text{and} \quad (7.2a)$$

$$\mathcal{F}_B \gtrsim \left( \frac{R}{R_L} \right)^{1/2} R^{-7/6} + \left( \frac{R}{R_L} \right)^{3/8} R^{-7/8} \left| \ln \left( 1 - \left( \frac{R}{R_L} \right)^{1/4} R^{-7/12} \right) \right|. \quad (7.2b)$$

Since  $R$  is always a multiple of  $R_L$ , for  $R > R_L$ , the bounds in (7.2) are smaller than the heuristic scaling laws (7.1). If the lower bounds are not sharp, then this would motivate the question of how to improve the bounds, which we now discuss with concluding remarks.

## 7.2. Conclusions

In this work we prove lower bounds on the mean temperature  $\overline{\langle T \rangle}$ , ((6.21) and (6.30)) and the mean heat flux out of the bottom boundary  $\mathcal{F}_B$  ((5.43) and (5.60)), for rotating uniform internally heated convection (IHC) in the limit of infinite Prandtl number. Using the fact that the momentum equation in Rayleigh-Bénard (RBC) and IHC is identical, we adapt estimates from Yan (2004) and Constantin *et al.* (1999) to prove the first Rayleigh and Ekman number dependent bounds on  $\overline{\langle T \rangle}$  and  $\mathcal{F}_B$  in IHC. By application of the auxiliary functional method, we prove bounds that apply to different regimes of buoyancy to rotation-dominated flows, summarised in fig. 8 and table 1. In addition to rigorous bounds, we demonstrate that the critical Rayleigh number for linear stability,  $R_L$ , asymptotically scales with the Ekman number as  $E^{-4/3}$  when the marginally stable states are steady. Furthermore, given the relation between  $E$  and the critical Rayleigh number for convection, we use heuristic arguments to propose a family of scaling laws for rotating IHC valid at arbitrary  $Pr$ .

In contrast to previous applications of the background field method, there are several unique features in the proofs of bounds in this work. Firstly, the background temperature fields have boundary layers of different widths for the proofs on  $\mathcal{F}_B$ , but not for  $\overline{\langle T \rangle}$ . In particular, when we use lemma 2 we find that  $\delta = \varepsilon^2$ , while when using lemma 3,  $\delta = \varepsilon^{5/2}$ . The relation from using lemma 2 (section 5.4) matches the predictions of our heuristic arguments (section 4). However, whether or not the background profiles are optimal remains unknown and should be addressed with numerical optimisation (Fantuzzi & Wynn 2016; Fantuzzi 2018; Fantuzzi *et al.* 2022). The bound obtained for  $\mathcal{F}_B$  in the slowly rotating regime (see regime I in fig. 8 and table 1) matches the best known bound for zero rotation, while this is not the case for the bound on  $\overline{\langle T \rangle}$ , but, both bounds only hold up to  $E \leq E_m = 41.4487$ . It would be interesting to investigate if a bound can be proven that holds for all  $E$  and matches bounds without rotation on  $\overline{\langle T \rangle}$  (Whitehead & Doering 2011a) and  $\mathcal{F}_B$  (Arslan & Rojas 2024) when  $E \rightarrow \infty$ . Additionally, from table 1, we realise that using lemma 3 for a bound on  $\mathcal{F}_B$  is not as good as for  $\overline{\langle T \rangle}$  because of the requirement that  $R > R_L \sim E^{-4/3}$ . It remains to be seen if one can find a bound on  $\mathcal{F}_B$  for  $E \leq R^{-n}$  where  $n < 3/4$ . The two lemmas give different bounds because they estimate the second derivative of the vertical velocity in different  $L^p$  norms and while lemma 2 is a pointwise estimate in  $z$ , lemma 3 is an integral estimate over the whole domain.

While rigorous demonstrations of the validity of the results at arbitrary  $Pr$  are not provided here, previous work in Tilgner (2022) outlines a strategy for extending bounds from  $Pr = \infty$  to finite  $Pr$  for RBC. The author achieves this under specific restrictions on  $E$  and a numerical approximation of a Greens' function, making the bound semi-analytic at best. A similar approach appears in Wang & Whitehead (2013) to extend bounds on RBC for stress-free boundaries from infinite  $Pr$  to arbitrary  $Pr$  in 3D. The barrier to adapting to IHC is the lack of a maximum principle on the temperature of the form  $\|T\|_\infty \leq c$ , where  $c = 1$  for RBC. A

proof of any maximum principle for IHC is not known. Therefore, at best, we can conjecture that akin to RBC, to highest order, the bounds in this work should hold for arbitrary  $Pr$ .

In considering turbulent convection subject to rotation, a question of interest is the behaviour in the limit of rapidly rotating convection. Rapidly rotating IHC could be investigated by taking the approach of the non-hydrostatic quasigeostrophic approximation (Julien *et al.* 1996; Sprague *et al.* 2006; Julien *et al.* 2016) to (2.1). It is worth noting that the bounds for the rapidly rotating limit in RBC apply to arbitrary  $Pr$ , making the results relevant for geophysical flows. However, for geophysical applications, in addition to rapid rotation, IHC in a spherical geometry is of importance. No rigorous work on the turbulent state of such a system has been carried out, and the change in the bounds with a variation in the geometry is an exciting avenue for future research.

For any result obtained with a bounding method, an important question is on the sharpness of the bounds. One way to gain insight into the sharpness of the bounds (1.2) and (1.3) is with numerical simulations. A numerical study of the parameter space would provide valuable insight into the nature of heat transport in uniform rotating IHC, especially given the lack of data, both numerical and experimental, on such a flow. Then, proof of better bounds, by moving away from quadratic auxiliary functionals, and hence the background method, would also answer the question of sharpness. In general, mathematical improvements are obtained in one of two ways: either by changes to the variational problem, such that the expressions for the bounds and the spectral constraint change, or by novel estimates of the flow quantities. The latter method is more mathematically challenging, but the first can be achieved with new physical insights. For example, given that additional constraints, like minimum and maximum principles, improve bounds for convection (Otto & Seis 2011; Arslan *et al.* 2021b), it would be interesting to see if information about rotating flows can be further leveraged to construct a variational problem from (2.1), that yields better bounds. Beyond the relation between the  $R_L$  and  $E$ , a trait of rotating flows is the Taylor-Proudman theorem, which could form the basis of an additional constraint which improves the bounds. Also, alternative auxiliary functionals might bear fruit in studying bounds on rotating convection. More concretely, the linear stability analysis reveals the importance of the vertical vorticity, and functionals that incorporate vorticity may provide insight into improved bounds, especially given the conjecture in Chernyshenko (2023) for the use of helicity in the auxiliary functional. Similar functionals appear in studies on nonlinear stability of rotating RBC (Galdi & Straughan 1985; Giacobbe & Mulone 2014).

As a final remark, recent work has highlighted novel results when the internal heating is non-uniform (Lepot *et al.* 2018; Bouillaut *et al.* 2022; Song *et al.* 2022; Arslan *et al.* 2024). The change in the physics or bounds due to distributed heating or cooling would be an interesting future line of research. From the perspective of the PDE, extending the setup in (2.1c) to arbitrary heating profiles would be the natural next step when studying bounds on the long-time behaviour of  $\langle T \rangle$  and  $\langle wT \rangle$ .

**Acknowledgments.** The author thanks Andrew Jackson for fruitful discussions, insights and for commenting on the manuscript and Fabian Burnman for reading and commenting on the manuscript.

**Funding.** The author acknowledges funding from the European Research Council (agreement no. 833848-UEMHP) under the Horizon 2020 program and the Swiss National Science Foundation (grant number 219247) under the MINT 2023 call.

**Declaration of interests.** The author reports no conflict of interest.



## Appendix A. Table of constants

For clarity in the proofs of the lower bounds on  $\mathcal{F}_B$  in (1.2) and  $\overline{\langle T \rangle}$  in (1.3), here we collate the constants that appear in the bounds. References to the precise equations where they appear are included.

Bound	Eq. number	Constant	Value
$\mathcal{F}_B$	(5.43)	$d_1$	$\frac{18-7\sqrt{3}}{36} \left( \frac{7\sqrt{6}}{16c_2} \right)^{2/3}$
	(5.43)	$d_2$	$\frac{1}{12} \left( \frac{1}{6} \right)^{1/12} \sqrt{\frac{21}{c_2}}$
	(5.43)	$d_3$	$\left( \frac{7\sqrt{6}}{12c_2} \right)^{1/3}$
	(5.43)	$d_4$	$\frac{18-7\sqrt{3}}{36} \left( \frac{49\sqrt{2}}{2c_2^2} \right)^{1/3}$
	(5.43)	$d_5$	$\frac{\sqrt{7}}{3} \left( \frac{9}{32\sqrt{2}c_2^5} \right)^{1/12}$
	(5.43)	$d_6$	$\left( \frac{392\sqrt{2}}{9c_2^2} \right)^{1/6}$
	(5.60)	$d_7$	$\frac{9\pi(18-7\sqrt{3})}{288}$
	(5.60)	$d_8$	$\frac{3\pi}{8} \left( \frac{8}{9\pi} \right)^{1/5}$
	(5.60)	$d_9$	$\left( \frac{9\pi}{8} \right)^{2/5}$
$\overline{\langle T \rangle}$	(6.21)	$d_{10}$	$\frac{2}{9} \left( \frac{7\sqrt{2}}{8c_2} \right)^{2/7}$
	(6.21)	$d_{11}$	$\frac{2}{9} \left( \frac{196}{c_2^2} \right)^{1/7}$
	(6.30)	$d_{12}$	$\frac{2}{9} \left( \frac{9\pi}{8} \right)^{1/3}$
	(6.30)	$d_{13}$	$\frac{1}{6}$

## REFERENCES

- AHLERS, G., GROSSMANN, S. & LOHSE, D. 2009 Heat transfer and large scale dynamics in turbulent Rayleigh–Bénard convection. *Reviews of Modern Physics* **81** (2), 503–537.
- ARSLAN, A., FANTUZZI, G., CRASKE, J. & WYNN, A. 2021a Bounds for internally heated convection with fixed boundary heat flux. *Journal of Fluid Mechanics* **992**, R1.
- ARSLAN, A., FANTUZZI, G., CRASKE, J. & WYNN, A. 2021b Bounds on heat transport for convection driven by internal heating. *Journal of Fluid Mechanics* **919**, A15.
- ARSLAN, A., FANTUZZI, G., CRASKE, J. & WYNN, A. 2023 Rigorous scaling laws for internally heated convection at infinite prandtl number. *Journal of Mathematical Physics* **64** (2), 023101.
- ARSLAN, A., FANTUZZI, G., CRASKE, J. & WYNN, A. 2024 Is downward conduction possible in turbulent convection driven by internal heating? *arXiv:2402.19240 [physics.flu-dyn]*.
- ARSLAN, A. & ROJAS, R. E. 2024 New bounds for heat transport in internally heated convection at infinite Prandtl number. *arXiv:2403.14407 [physics.flu-dyn]*.
- AURNOU, J. M., HORN, S. & JULIEN, K. 2020 Connections between nonrotating, slowly rotating, and rapidly rotating turbulent convection transport scalings. *Physical Review Research* **2** (4), 043115.
- BARKER, A. J., DEMPSEY, A. M. & LITHWICK, Y. 2014 Theory and simulations of rotating convection. *The Astrophysical Journal* **791** (1), 13.
- BOUBNOV, B. M. & GOLITSYN, G. S. 2012 *Convection in rotating fluids*, , vol. 29. Springer Science & Business Media.

- BOULLAUT, V., FLESSELLES, B., MIQUEL, B., AUMAÎTRE, S. & GALLET, B. 2022 Velocity-informed upper bounds on the convective heat transport induced by internal heat sources and sinks. *Philosophical Transactions of the Royal Society A* **380** (2225), 20210034.
- BUSSE, F. H. 1970 Bounds for turbulent shear flow. *Journal of Fluid Mechanics* **41** (1), 219–240.
- CHANDRASEKHAR, S. 1961 *Hydrodynamic and hydromagnetic stability*. Oxford University Press.
- CHERNYSHENKO, S. 2022 Relationship between the methods of bounding time averages. *Philosophical Transactions of the Royal Society A* **380** (1), 20210044.
- CHERNYSHENKO, S. 2023 Background flow hidden in a bound for nusselt number. *Physica D: Nonlinear Phenomena* **445**, 133641.
- CHERNYSHENKO, S., GOULART, P. J., HUANG, D. & PAPACHRISTODOULOU, A. 2014 Polynomial sum of squares in fluid dynamics: a review with a look ahead. *Philosophical Transactions of the Royal Society A* **372** (2020), 20130350.
- CONSTANTIN, P. 1994 Geometric statistics in turbulence. *SIAM Review*. **36** (1), 73–98.
- CONSTANTIN, P. & DOERING, C. R. 1995 Variational bounds on energy dissipation in incompressible flows. II. Channel flow. *Physical Review E* **51** (4), 3192–3198.
- CONSTANTIN, P., HALLSTROM, C. & PUTKARADZE, V. 2001 Logarithmic bounds for infinite prandtl number rotating convection. *Journal of Mathematical Physics* **42** (2), 773–783.
- CONSTANTIN, P., HALLSTROM, C. & PUTKARADZE, V. 1999 Heat transport in rotating convection. *Physica D: Nonlinear Phenomena* **125** (3–4), 275–284.
- CREYSSELS, M. 2020 Model for classical and ultimate regimes of radiatively driven turbulent convection. *Journal of Fluid Mechanics* **900**, A39.
- CREYSSELS, M. 2021 Model for thermal convection with uniform volumetric energy sources. *Journal of Fluid Mechanics* **919**, A13.
- CURRIE, L. K., BARKER, A. J., LITHWICK, Y. & BROWNING, M. K. 2020 Convection with misaligned gravity and rotation: Simulations and rotating mixing length theory. *Monthly Notices of the Royal Astronomical Society* **493** (4), 5233–5256.
- DAVIS, S. H. 1969 On the principle of exchange of stabilities. *Proceedings of the Royal Society of London. Series A, Mathematical and Physical Sciences* **310** (1502), 341–358.
- DING, Z. & MARENSI, E. 2019 Upper bound on angular momentum transport in taylor-couette flow. *Physical Review E* **100** (6), 063109.
- DOERING, C. R. 2020 Turning up the heat in turbulent thermal convection. *Proceedings of the National Academy of Sciences* **117** (18), 9671–9673.
- DOERING, C. R. & CONSTANTIN, P. 1992 Energy dissipation in shear driven turbulence. *Physical Review Letters* **69** (11), 1648.
- DOERING, C. R. & CONSTANTIN, P. 1994 Variational bounds on energy dissipation in incompressible flows: Shear flow. *Physical Review E* **49** (5), 4087–4099.
- DOERING, C. R. & CONSTANTIN, P. 1996 Variational bounds on energy dissipation in incompressible flows. III. Convection. *Physical Review E* **53** (6), 5957–5981.
- DOERING, C. R. & CONSTANTIN, P. 2001 On upper bounds for infinite Prandtl number convection with or without rotation. *Journal of Mathematical Physics* **42** (2), 784–795.
- DOERING, C. R., OTTO, F. & REZNIKOFF, M. G. 2006 Bounds on vertical heat transport for infinite Prandtl number Rayleigh–Bénard convection. *Journal of Fluid Mechanics* **560**, 229–241.
- ECKE, R. E. & SHISHKINA, O. 2023 Turbulent rotating rayleigh–bénard convection. *Annual review of fluid mechanics* **55**, 603–638.
- FANTUZZI, G. 2018 Bounds for Rayleigh–Bénard convection between free-slip boundaries with an imposed heat flux. *Journal of Fluid Mechanics* **837**, R5.
- FANTUZZI, G., ARSLAN, A. & WYNN, A. 2022 The background method: Theory and computations. *Philosophical Transactions of the Royal Society A* **380** (1), 20210038.
- FANTUZZI, G. & WYNN, A. 2016 Optimal bounds with semidefinite programming: An application to stress-driven shear flows. *Physical Review E* **93** (4), 043308.
- GALDI, G. P. & STRAUGHAN, B. 1985 A nonlinear analysis of the stabilizing effect of rotation in the Bénard problem. *Proceedings of the Royal Society of London. A. Mathematical and Physical Sciences* **402** (1823), 257–283.
- GIACOBBE, A. & MULONE, G. 2014 Stability in the rotating benard problem and its optimal lyapunov functions. *Acta Applicandae Mathematicae* **132**, 307–320.
- GLATZMAIER, G. 2013 *Introduction to modeling convection in planets and stars: Magnetic field, density stratification, rotation*. Princeton University Press.

- GOLUSKIN, D. 2016 *Internally heated convection and Rayleigh–Bénard convection*. Springer.
- GOLUSKIN, D. & VAN DER POEL, E. P. 2016 Penetrative internally heated convection in two and three dimensions. *Journal of Fluid Mechanics* **791**.
- GOLUSKIN, D. & SPIEGEL, E. A. 2012 Convection driven by internal heating. *Physics Letters A* **377** (1-2), 83–92.
- GREENSPAN, H. P. 1968 *The theory of rotating fluids*. Cambridge University Press.
- GROOMS, I., JULIEN, K., WEISS, J. B. & KNOBLOCH, E. 2010 Model of convective Taylor columns in rotating Rayleigh–Bénard convection. *Physical Review Letters* **104** (22), 224501.
- GROOMS, I. & WHITEHEAD, J. P. 2014 Bounds on heat transport in rapidly rotating Rayleigh–Bénard convection. *Nonlinearity* **28** (1), 29.
- GROSSMANN, S. & LOHSE, D. 2000 Scaling in thermal convection: a unifying theory. *Journal of Fluid Mechanics* **407**, 27–56.
- GUERVILLY, C. & CARDIN, P. 2016 Subcritical convection of liquid metals in a rotating sphere using a quasi-geostrophic model. *Journal of Fluid Mechanics* **808**, 61–89.
- GUZMÁN, A. J. A., MADONIA, M., CHENG, J. S., OSTILLA-MÓNICO, R., CLERCX, H. J. H. & KUNNEN, R. P. J. 2020 Competition between Ekman plumes and vortex condensates in rapidly rotating thermal convection. *Physical Review Letters* **125** (21), 214501.
- HADJERCI, G., BOULLAUT, V., MIQUEL, B. & GALLET, B. 2024 Rapidly rotating radiatively driven convection: experimental and numerical validation of the ‘geostrophic turbulence’ scaling predictions, arXiv: 2401.16200.
- HERANT, M., BENZ, W., HIX, W. R., FRYER, C. L. & COLGATE, S. A. 1994 Inside the supernova: A powerful convective engine. *Astrophysical Journal, Part 1 (ISSN 0004-637X)*, vol. 435, no. 1, p. 339–361 **435**, 339–361.
- HERRON, I. H. 2003 On the principle of exchange of stabilities in Rayleigh–Bénard convection, ii-no-slip boundary conditions. *Annali dell’Università di Ferrara* **49**, 169–182.
- HOWARD, L. N. 1963 Heat transport by turbulent convection. *Journal of Fluid Mechanics* **17** (3), 405–432.
- JONES, C. A. & SCHUBERT, G. 2015 Thermal and compositional convection in the outer core. *Treatise in Geophysics, Core Dynamics* **8**, 131–185.
- JONES, C. A., SOWARD, A. M. & MUSSA, A. I. 2000 The onset of thermal convection in a rapidly rotating sphere. *Journal of Fluid Mechanics* **405**, 157–179.
- JULIEN, K., AURNOU, J. M., CALKINS, M. A., KNOBLOCH, E., MARTI, P., STELLMACH, S. & VASIL, G. M. 2016 A nonlinear model for rotationally constrained convection with Ekman pumping. *Journal of Fluid Mechanics* **798**, 50–87.
- JULIEN, K., LEGG, S., MCWILLIAMS, J. & WERNE, J. 1996 Rapidly rotating turbulent Rayleigh–Bénard convection. *Journal of Fluid Mechanics* **322**, 243–273.
- JULIEN, K., RUBIO, A. M., GROOMS, I. & KNOBLOCH, E. 2012 Statistical and physical balances in low Rossby number Rayleigh–Bénard convection. *Geophysical & Astrophysical Fluid Dynamics* **106** (4-5), 392–428.
- KAPLAN, E. J., SCHAEFFER, N., VIDAL, J. & CARDIN, P. 2017 Subcritical thermal convection of liquid metals in a rapidly rotating sphere. *Physical Review Letters* **119** (9), 094501.
- KING, E. M., STELLMACH, S. & BUFFETT, B. 2013 Scaling behaviour in Rayleigh–Bénard convection with and without rotation. *Journal of Fluid Mechanics* **717**, 449–471.
- KING, E. M., STELLMACH, S., NOIR, J., HANSEN, U. & AURNOU, J. M. 2009 Boundary layer control of rotating convection systems. *Nature* **457** (7227), 301–304.
- KNOBLOCH, E. 1998 Rotating convection: recent developments. *International journal of engineering science* **36** (12-14), 1421–1450.
- KUMAR, A. 2022 Geometrical dependence of optimal bounds in Taylor–Couette flow. *Journal of Fluid Mechanics* **948**, A11.
- KUMAR, A., ARSLAN, A., FANTUZZI, G., CRASKE, J. & WYNN, A. 2022 Analytical bounds on the heat transport in internally heated convection. *Journal of Fluid Mechanics* **938**, A26.
- LEPOT, S., AUMAÎTRE, S. & GALLET, B. 2018 Radiative heating achieves the ultimate regime of thermal convection. *Proceedings of the National Academy of Sciences of the U.S.A.* **115** (36), 8937–8941.
- LU, L., DOERING, C. R. & BUSSE, F. H. 2004 Bounds on convection driven by internal heating. *Journal of Mathematical Physics* **45** (7), 2967–2986.
- MALKUS, W. V. R. 1954 The heat transport and spectrum of thermal turbulence. *Proceedings of the Royal Society A* **225** (1161), 196–212.

- MULYUKOVA, E. & BERCOVICI, D. 2020 Mantle convection in terrestrial planets. *Oxford Research Encyclopedia of Planetary Sciences*.
- NOBILI, C. 2023 The role of boundary conditions in scaling laws for turbulent heat transport. *Mathematics in Engineering* **5** (1), 1–41.
- OTTO, F. & SEIS, C. 2011 Rayleigh–Bénard convection: Improved bounds on the Nusselt number. *Journal of Mathematical Physics* **52** (8), 083702.
- PACHEV, B., WHITEHEAD, J. P., FANTUZZI, G. & GROOMS, I. 2020 Rigorous bounds on the heat transport of rotating convection with Ekman pumping. *Journal of Mathematical Physics* **61** (2), 023101.
- PLUMLEY, M. & JULIEN, K. 2019 Scaling laws in rayleigh–bénard convection. *Earth and Space Science* **6** (9), 1580–1592.
- PRIESTLEY, C. H. B. 1954 Vertical heat transfer from impressed temperature fluctuations. *Australian Journal of Physics* **7** (1), 202–209.
- RADICE, D., OTT, C. D., ABDIKAMALOV, E., COUCH, S. M., HAAS, R. & SCHNETTER, E. 2016 Neutrino-driven convection in core-collapse supernovae: high-resolution simulations. *The Astrophysical Journal* **820** (1), 76.
- ROBERTS, P. H. 1967 Convection in horizontal layers with internal heat generation. theory. *Journal of Fluid Mechanics* **30** (1), 33–49.
- ROBERTS, P. H. 1968 On the thermal instability of a rotating-fluid sphere containing heat sources. *Philosophical Transactions of the Royal Society of London A* **263** (1136), 93–117.
- ROSA, R. M. S. & TEMAM, R. M. 2022 Optimal minimax bounds for time and ensemble averages of dissipative infinite-dimensional systems with applications to the incompressible Navier–Stokes equations. *Pure and Applied Functional Analysis* **7** (1), 327–355.
- ROSSBY, H. T. 1969 A study of Bénard convection with and without rotation. *Journal of Fluid Mechanics* **36** (2), 309–335.
- SCHUBERT, G. 2015 *Treatise on geophysics*. Elsevier.
- SCHUBERT, G., TURCOTTE, D. L. & OLSON, P. 2001 *Mantle convection in the Earth and planets*. Cambridge University Press.
- SCHUMACHER, J. & SREENIVASAN, K. R. 2020 Colloquium: Unusual dynamics of convection in the sun. *Rev. Mod. Phys.* **92**, 041001.
- SONG, B., FANTUZZI, G. & TOBASCO, I. 2022 Bounds on heat transfer by incompressible flows between balanced sources and sinks. *Physica D: Nonlinear Phenomena* p. 133591.
- SONG, J., SHISHKINA, O. & ZHU, X. 2024 Scaling regimes in rapidly rotating thermal convection at extreme rayleigh numbers. *Journal of Fluid Mechanics* **984**, A45.
- SPIEGEL, E. A. 1963 A generalization of the mixing-length theory of turbulent convection. *The Astrophysical Journal* **138**, 216.
- SPRAGUE, M., JULIEN, K., KNOBLOCH, E. & WERNE, J. 2006 Numerical simulation of an asymptotically reduced system for rotationally constrained convection. *Journal of Fluid Mechanics* **551**, 141–174.
- STELLMACH, S., LISCHPER, M., JULIEN, K., VASIL, G., CHENG, J. S., RIBEIRO, A., KING, E. M. & AURNOU, J. M. 2014 Approaching the asymptotic regime of rapidly rotating convection: boundary layers versus interior dynamics. *Physical review letters* **113** (25), 254501.
- STEVENS, R. J. A. M., VAN DER POEL, E. P., GROSSMANN, S. & LOHSE, D. 2013 The unifying theory of scaling in thermal convection: the updated prefactors. *Journal of Fluid Mechanics* **730**, 295–308.
- STEVENSON, D. J. 1979 Turbulent thermal convection in the presence of rotation and a magnetic field: A heuristic theory. *Geophysical & Astrophysical Fluid Dynamics* **12** (1), 139–169.
- STRAUGHAN, B. 2013 *The energy method, stability, and nonlinear convection*, , vol. 91. Springer Science & Business Media.
- TILGNER, A. 2022 Bounds for rotating rayleigh–bénard convection at large prandtl number. *Journal of Fluid Mechanics* **930**, A33.
- TOBASCO, I., GOLUSKIN, D. & DOERING, C. R. 2018 Optimal bounds and extremal trajectories for time averages in nonlinear dynamical systems. *Physics Letters A* **382** (6), 382–386, arXiv: 1705.07096.
- VERONIS, G. 1959 Cellular convection with finite amplitude in a rotating fluid. *Journal of Fluid Mechanics* **5** (3), 401–435.
- VOROBIEFF, P. & ECKE, R. E. 2002 Turbulent rotating convection: an experimental study. *Journal of Fluid Mechanics* **458**, 191–218.
- WANG, Q., LOHSE, D. & SHISHKINA, O. 2020 Scaling in internally heated convection: a unifying theory. *Geophysical Research Letters* **47**, e2020GL091198.
- WANG, X. 2007 Asymptotic behavior of the global attractors to the Boussinesq system for Rayleigh–Bénard

- convection at large Prandtl number. *Communications on Pure and Applied Mathematics* **60** (9), 1293–1318.
- WANG, X. & WHITEHEAD, J. P. 2013 A bound on the vertical transport of heat in the ‘ultimate’ state of slippery convection at large prandtl numbers. *Journal of Fluid Mechanics* **729**, 103–122.
- WHITEHEAD, J. P. & DOERING, C. R. 2011*a* Internal heating driven convection at infinite Prandtl number. *Journal of Mathematical Physics* **52** (9), 093101.
- WHITEHEAD, J. P. & DOERING, C. R. 2011*b* Ultimate state of two-dimensional Rayleigh–Bénard convection between free-slip fixed-temperature boundaries. *Physical Review Letters* **106** (24), 244501.
- WHITEHEAD, J. P. & DOERING, C. R. 2012 Rigid bounds on heat transport by a fluid between slippery boundaries. *Journal of Fluid Mechanics* **707**, 241–259.
- YAN, X. 2004 On limits to convective heat transport at infinite Prandtl number with or without rotation. *Journal of Mathematical Physics* **45** (7), 2718–2743.